

FTUV-02-0411

IFIC-02-09

Pinch Technique and the Batalin-Vilkovisky formalism

Daniele Binosi and Joannis Papavassiliou

*Departamento de Física Teórica and IFIC,
Centro Mixto, Universidad de Valencia-CSIC,
E-46100, Burjassot, Valencia, Spain**

(Dated: April 11, 2002)

Abstract

In this paper we take the first step towards a non-diagrammatic formulation of the Pinch Technique. In particular we proceed into a systematic identification of the parts of the one-loop and two-loop Feynman diagrams that are exchanged during the pinching process in terms of unphysical ghost Green's functions; the latter appear in the standard Slavnov-Taylor Identity satisfied by the tree-level and one-loop three-gluon vertex. This identification allows for the consistent generalization of the intrinsic Pinch Technique to two loops, through the collective treatment of entire sets of diagrams, instead of the laborious algebraic manipulation of individual graphs, and sets up the stage for the generalization of the method to all orders. We show that the task of comparing the effective Green's functions obtained by the Pinch Technique with those computed in the Background Field Method Feynman gauge is significantly facilitated when employing the powerful quantization framework of Batalin and Vilkovisky. This formalism allows for the derivation of a set of useful non-linear identities, which express the Background Field Method Green's functions in terms of the conventional (quantum) ones and auxiliary Green's functions involving the background source and the gluonic anti-field; these latter Green's functions are subsequently related by means of a Schwinger-Dyson type of equation to the ghost Green's functions appearing in the aforementioned Slavnov-Taylor Identity.

PACS numbers: 11.15.Bt, 11.55.Fv, 12.38.Bx, 14.70.Dj

*Electronic address: Daniele.Binosi@uv.es; Joannis.Papavassiliou@uv.es

I. INTRODUCTION

The Pinch Technique (PT) [1, 2, 3] is a diagrammatic method which exploits the underlying symmetries encoded in a *physical* amplitude such as an S -matrix element, in order to construct effective Green's functions with special properties. The aforementioned symmetries, even though they are always present, they are usually concealed by the gauge-fixing procedure. The PT makes them manifest by means of a fixed algorithm, which does *not* depend on the gauge-fixing scheme one uses in order to quantize the theory, *i.e.*, regardless of the set of Feynman rules used when writing down the S -matrix element. The PT exploits the elementary Ward Identities (WIs) triggered by the longitudinal momenta appearing inside Feynman diagrams in order to enforce massive cancellations. The realization of these cancellations mixes non-trivially contributions stemming from diagrams of different kinematic nature (propagators, vertices, boxes). Thus, a given physical amplitude is reorganized into sub-amplitudes, which have the same kinematic properties as conventional n -point functions and, in addition, are endowed with desirable physical properties. Most importantly, at one- and two-loop order they are independent of the gauge-fixing parameter, satisfy naive (ghost-free) tree-level WIs instead of the usual Slavnov-Taylor identities (STIs) [4, 5], and contain only physical thresholds [6, 7].

It is clear by now that an intimate connection exists between the PT and the Background Field Method (BFM) [8, 9, 10, 11, 12, 13, 14, 15, 16, 17, 18]. The BFM is a special gauge-fixing procedure, implemented at the level of the generating functional. In particular, it preserves the symmetry of the action under ordinary gauge transformations with respect to the background (classical) gauge field \widehat{A}_μ , while the quantum gauge fields A_μ appearing in the loops transform homogeneously under the gauge group, *i.e.*, as ordinary matter fields which happened to be assigned to the adjoint representation [19]. As a result of the background gauge symmetry, the BFM n -point functions $\langle 0|T \left[\widehat{A}_{\mu_1}(x_1)\widehat{A}_{\mu_2}(x_2)\dots\widehat{A}_{\mu_n}(x_n) \right] |0\rangle$ satisfy naive QED-like WIs, but (unlike QED) depend explicitly on the quantum gauge-fixing parameter ξ_Q used to define the tree-level propagators of the quantum gluons. It turns out that at one-loop order, both in QCD and in the Electroweak sector of the Standard Model, the gauge-fixing parameter-independent effective n -point functions constructed by means of the PT (starting from any gauge-fixing scheme) coincide with the corresponding background n -point functions when the latter are computed at the special value $\xi_Q = 1$ (BFM Feynman

gauge) [20, 21, 22] . As was shown in detail in [23, 24], this correspondence *persists* at two loops in the case of QCD.

One of the most pressing questions in this context is whether one can extend the PT algorithm to all orders in perturbation theory, thus achieving the systematic construction of effective n -point functions displaying the aforementioned characteristic features. To accomplish this it is clear that one needs to go beyond the diagrammatic manipulations employed until now, and resort to a more formal procedure. Indeed, one disadvantage of the PT method is the fact that the constructions rely heavily on algebraic operations inside individual Feynman graphs. Even though these operations proceed according to well-defined guiding principles which have been spelled out in various occasions in the existing literature, any attempt to apply them to higher orders would constitute an operationally hopeless task. But even if the resulting re-shuffling of terms among the Feynman graphs would eventually lead to a well-defined answer, additional effort would be required in order to compare this unique answer to the BFM n -point functions, and to verify whether the correspondence mentioned above persists to all orders.

To ameliorate this situation, in this paper we take a first step towards a non-diagrammatic formulation of the PT procedure. In particular we proceed into a systematic identification of the parts of the one-loop and two-loop Feynman diagrams that are shuffled around during the pinching process in terms of well-defined field-theoretical objects, namely the ghost Green's functions which appear in the STIs satisfied by the tree-level and one-loop three-gluon vertex [25]. This constitutes an important step because it enables one to go beyond the current diagrammatic implementation of the pinching procedure by means of tree-level WIs appearing in individual graphs, allowing instead the collective treatment of entire sets of diagrams, and sets up the stage for the generalization of the method to all orders [26]. Thus, at least at one- and two-loops, the final PT answer for a given effective Green's function is obtained from the original Green's function by adding (or subtracting) a well-defined set of contributions identified when the relevant STIs have been triggered *inside* the Green's function under consideration.

The conventional derivation of the STIs using the Becchi-Rouet-Stora-Tyutin (BRST) transformations [27, 28, 29] and the definition of the building blocks in terms of unphysical ghost-Green's functions is in itself a text-book exercise [30]. But in addition, we will carry out the derivation of the very same STIs using the Batalin-Vilkovisky (BV) formalism [31,

32]. In particular, the STIs written in the context of the BV are realized by means of auxiliary unphysical Green's functions, which involve ghosts and anti-fields; the latter are characteristic of the BV formalism, and do not appear in the conventional formulation of the gauge theory. Of course, since the STI in both formulation involves the same original Green's function, namely it is the STI of the three-gluon vertex, the building blocks appearing in the two formulations—conventional and BV—must be related. It turns out that this indeed the case, as we will see in detail in Section II. The reason for going through this exercise is because thusly one may take advantage of an important ingredient furnished by the BV formulation, which facilitates significantly the comparison of the PT results with those of the BFM. Specifically using the formulation of the BFM within the BV formalism, one can derive non-trivial identities relating the BFM n -point functions to the corresponding conventional n -point functions in the covariant renormalizable gauges, to all orders in perturbation theory. These identities, which we will call Background-Quantum identities (BQIs) in what follows, have been derived for the first time in the context of the Standard Model in [33, 34]. The quantities appearing in these BQIs are Green's functions involving anti-fields and background sources, introduced in the BFM formulation. It turns out that the auxiliary Green's functions appearing in the STIs and those appearing in the BQIs, are related by simple expressions, a fact which allows for a direct comparison of the PT and BFM Green's functions. Notice that the BV formalism furnishes exact Feynman rules for the perturbative construction of all aforementioned unphysical, auxiliary Green's function, appearing in the STIs and the BQIs.

It is conceptually very important to emphasize the logical succession of the steps involved in this entire construction: One begins with a massless Yang-Mills theory, such as QCD, formulated in the conventional way, *i.e.*, with a linear covariant gauge-fixing term of the form $\frac{1}{2\xi} (\partial^\mu A_\mu^a)^2$, together with the corresponding ghost-sector, introduced by the standard Faddeev-Popov construction; at this stage this theory knows nothing about neither the BFM nor the anti-fields appearing in the BV formulation. Exploiting only the STIs, derived by virtue of the BRST symmetry and formulated in the language of the conventional theory, *i.e.*, expressed solely in terms of objects definable within this theory, one can reach after a well-defined set of steps the PT answer. The most expeditious way for comparing this answer to the corresponding BFM Green's function is the following: one derives the aforementioned STIs using the BV formalism, *i.e.* one translates the STIs from the normal language to the

BV language; the reason is that thusly one can exploit the identities – derivable in the BV language – relating the BFM Green’s functions to the normal ones.

The paper is organized as follows: In Section II we present a brief introduction to the BV formalism, providing the minimum amount of information needed for establishing notation and arriving at the relevant generating functional. In Section III we derive the necessary ingredients following standard manipulations: In particular we derive the STIs within the BV, as well as the BQIs for various cases. In addition, we derive a Schwinger-Dyson type of identity relating the building blocks appearing in the STIs to those appearing in the BQIs; to the best of our knowledge this relation appears for the first time in the literature. In Section IV we review the PT construction, and put to work the formalism derived above. Even though the PT part is standard, this section provides a distilled review of the PT method, and serves as a simple testing-ground for establishing the desired connections between the two formalisms. In Section V we present the two-loop construction, where the connections established are further scrutinized, within a far more complex context. In Section VI we present an entirely new result, even from the point of view of conventional PT, namely the two-loop generalization of the intrinsic PT construction. In particular, we will show how the judicious organization of entire sets of two-loop diagrams, together with the use of the STI for the one-loop three-gluon vertex, leads to the PT answer for the two-loop effective gluon self-energy. Finally, in Section VII we present our conclusions.

II. THE BATALIN-VILKOVISKY FORMALISM

In this section we will briefly review the most salient features of the BV formalism [31, 32], concentrating to its application to the case of massless Yang-Mills theories.

The (gauge fixed) Yang-Mills Lagrangian density will be given by

$$\mathcal{L}_{\text{YM}} = \mathcal{L}_{\text{I}} + \mathcal{L}_{\text{GF}} + \mathcal{L}_{\text{FPG}}, \quad (2.1)$$

with \mathcal{L}_{I} the usual gauge invariant $SU(N)$ Yang-Mills Lagrangian,

$$\mathcal{L}_{\text{I}} = -\frac{1}{4}F_{\mu\nu}^a F^{a\mu\nu} + \bar{\psi} (i\not{D} - m) \psi, \quad (2.2)$$

where

$$F_{\mu\nu}^a = \partial_\mu A_\nu^a - \partial_\nu A_\mu^a + gf^{abc} A_\mu^b A_\nu^c, \quad (2.3)$$

g is the gauge coupling, and D_μ is the covariant derivative defined as

$$D_\mu = \partial_\mu - igT^a A_\mu^a. \quad (2.4)$$

The covariant gauge fixing and Faddeev-Popov term $\mathcal{L}_{\text{GF}} + \mathcal{L}_{\text{FPG}}$ will be chosen to have the form

$$\mathcal{L}_{\text{GF}} + \mathcal{L}_{\text{FPG}} = -\frac{1}{2}\xi (B^a)^2 + B^a \partial^\mu A_\mu^a - \bar{c}^a \partial^\mu (\partial_\mu c^a - gf^{abc} A_\mu^b c^c). \quad (2.5)$$

The B^a are auxiliary, non-dynamical fields, since they have a quadratic term without derivatives (and as such they are not propagating). They represent the so-called Nakanishi-Lautrup Lagrange multiplier for the gauge condition, and they are usually eliminated through the corresponding Gaussian integration in the path integral, giving rise to the usual gauge fixing term

$$\mathcal{L}_{\text{GF}} = \frac{1}{2\xi} (\partial^\mu A_\mu^a)^2. \quad (2.6)$$

The starting point of the BV formalism is the introduction of an *external* field – called anti-field – $\Phi^{*,n}$ for each field Φ^n appearing in the Lagrangian. In particular, here Φ^n represent generically any of the fields $A_\mu^a, c^a, \bar{c}^a, \psi, \bar{\psi}$ and B^a appearing in Eq.(2.1). The anti-fields $\Phi^{*,n}$ will carry the same Bose/Fermi statistic of the corresponding field Φ^n and a ghost number such that

$$gh\{\Phi^{*,n}\} = -gh\{\Phi^n\} - 1. \quad (2.7)$$

Thus, since the ghost number is equal to 1 for the ghost fields c^a , to -1 for the anti-ghost fields \bar{c}^a , and zero for the other fields, one has the assignment

$$gh\{A_\mu^{*,a}, c^{*,a}, \bar{c}^{*,a}, \psi^*, \bar{\psi}^*\} = \{-1, -2, 0, -1, -1\}. \quad (2.8)$$

The original gauge invariant Lagrangian is then supplemented with a term coupling to the anti-fields $\Phi^{*,n}$ with the BRST variation of Φ^n , giving the modified Lagrangian

$$\begin{aligned} \mathcal{L}_{\text{BV}} &= \mathcal{L}_{\text{I}} + \mathcal{L}_{\text{BRST}} \\ &= \mathcal{L}_{\text{I}} + \sum_n \Phi^{*,n} s\Phi^n, \end{aligned} \quad (2.9)$$

with s the BRST operator, and

$$\begin{aligned} sA_\mu^a &= \partial_\mu c^a - gf^{abc} A_\mu^b c^c, & sc^a &= -\frac{1}{2}gf^{abc} c^b c^c, \\ s\psi &= igc^a T^a \psi, & s\bar{\psi} &= -ig\bar{\psi} T^a c^a, \\ s\bar{c}^a &= B^a, & sB^a &= 0. \end{aligned} \quad (2.10)$$

The action $\mathbb{I}^{(0)}[\Phi, \Phi^*]$ built up from the new Lagrangian \mathcal{L}_{BV} , will then satisfy the *master equation*

$$\int d^4x \left[\frac{\delta \mathbb{I}^{(0)}}{\delta \Phi^{*,n}} \frac{\delta \mathbb{I}^{(0)}}{\delta \Phi^n} \right] = 0, \quad (2.11)$$

which is just a consequence of the BRST invariance of the action and of the nilpotency of the BRST operator.

Since the anti-fields are external fields, we must constrain them to suitable values before we can use the action $\mathbb{I}^{(0)}$ in the calculation of S -matrix elements. To this purpose one introduces an arbitrary fermionic functional $\Psi[\Phi]$ (with $gh\{\Psi[\Phi]\} = -1$) such that

$$\Phi^{*,n} = \frac{\delta \Psi[\Phi]}{\delta \Phi^n}. \quad (2.12)$$

Then the action becomes

$$\begin{aligned} \mathbb{I}^{(0)}[\Phi, \delta \Psi / \delta \Phi] &= \mathbb{I}^{(0)}[\Phi] + (s\Phi^n) \frac{\delta \Psi[\Phi]}{\delta \Phi^n} \\ &= \mathbb{I}^{(0)}[\Phi] + s\Psi[\Phi], \end{aligned} \quad (2.13)$$

i.e., it is equivalent to the gauge fixed action of the Yang-Mills theory under scrutiny, since we can choose the fermionic functional Ψ to satisfy

$$s\Psi[\Phi] = \int d^4x (\mathcal{L}_{\text{GF}} + \mathcal{L}_{\text{FPG}}). \quad (2.14)$$

The fermionic functional Ψ is often referred to as the gauge fixing fermion.

Moreover, the auxiliary fields B^a and the anti-ghost anti-fields $\bar{c}^{*,a}$ have linear BRST transformations, so that they form a so called *trivial pair* [35]: they enter, together with their anti-fields, bilinearly in the action

$$\mathbb{I}^{(0)}[\Phi, \Phi^*] = \mathbb{I}_{\text{min}}^{(0)}[A_\mu^a, c^a, A_\mu^{*,a}, c^{*,a}] - B^a \bar{c}^{*,a}. \quad (2.15)$$

The last term has no effect on the master equation, which will be in fact satisfied by the *minimal* action $\mathbb{I}_{\text{min}}^{(0)}$ alone. In what follows we will restrict our considerations to the minimal action (which depends on the *minimal variables* $A_\mu^a, c^a, A_\mu^{*,a}, c^{*,a}$), dropping the corresponding subscript.

It is well known that the BRST symmetry is crucial for providing the unitarity of the S -matrix and the gauge independence of physical observables; thus it must be implemented

in the theory to all orders, not only at the classical level. This is provided by establishing the quantum corrected version of Eq.(2.11), in the form of the STI functional

$$\begin{aligned}
\mathcal{S}(\mathbb{I})[\Phi, \Phi^*] &= \int d^4x \left[\frac{\delta \mathbb{I}}{\delta \Phi^{*,n}} \frac{\delta \mathbb{I}}{\delta \Phi^n} \right] \\
&= \int d^4x \left[\frac{\delta \mathbb{I}}{\delta A_\mu^{*,a}} \frac{\delta \mathbb{I}}{\delta A_\mu^a} + \frac{\delta \mathbb{I}}{\delta c^{*,a}} \frac{\delta \mathbb{I}}{\delta c^a} + \frac{\delta \mathbb{I}}{\delta \psi^*} \frac{\delta \mathbb{I}}{\delta \bar{\psi}} + \frac{\delta \mathbb{I}}{\delta \bar{\psi}} \frac{\delta \mathbb{I}}{\delta \psi^*} \right] \\
&= 0,
\end{aligned} \tag{2.16}$$

where $\mathbb{I}[\Phi, \Phi^*]$ is now the effective action. Eq.(2.16) gives rise to the complete set of non linear STIs at all orders in the perturbative theory, via the repeated application of functional differentiation. Notice that $gh\{\mathcal{S}(\mathbb{I})\} = +1$ and that Green's functions with non-zero ghost charge vanish, since it is a conserved quantity. This implies that for getting non-zero identities it is necessary to differentiate the expression (2.16) with respect to one ghost field (ghost charge +1) or with respect to two ghost fields and one anti-field (ghost charge $+2 - 1 = +1$ again). For example, for deriving the STI satisfied by the three-gluon vertex, one has to differentiate Eq.(2.16) with respect to two gluon fields and one ghost field (see Section III A below).

A technical remark is in order here. Recall that we have chosen to work with the minimal generating functional \mathbb{I} , from which the trivial pair $(B^a, \bar{c}^{*,a})$ has been removed [35, 36]. In the case of a linear gauge fixing as the one at hands, this is equivalent to working with the “reduced” functional \mathbb{I} , defined by subtracting from the complete generating functional \mathbb{I}^c the local term $\int d^4x \mathcal{L}_{\text{GF}}$ corresponding to the gauge-fixing part of the Lagrangian. One should then keep in mind that the Green's functions generated by the minimal effective action \mathbb{I} or the complete one \mathbb{I}^c are not equal [33]. At tree-level, one has for example that

$$\begin{aligned}
\mathbb{I}_{A_\mu^a A_\nu^b}^{(0)}(q) &= \mathbb{I}_{A_\mu^a A_\nu^b}^{C(0)}(q) + \frac{1}{\xi} q_\mu q_\nu \\
&= -i\delta^{ab} q^2 P_{\mu\nu}(q),
\end{aligned} \tag{2.17}$$

where $P_{\mu\nu} = g_{\mu\nu} - q_\mu q_\nu / q^2$ is the dimensionless transverse projector; at higher orders the difference depends only on the renormalization of the gluon field and of the gauge parameter (and, as such, is immaterial for our purposes).

Another important ingredient of the construction we carry out in what follows is to write down the STI functional in the BFM. For doing this we introduce a classical vector field Ω_μ^a which carries the same quantum numbers as the gluon but ghost charge +1. We

then implement the equations of motion of the background fields at the quantum level by extending the BRST symmetry to them through the equations

$$s\widehat{A}_\mu^a = \Omega_\mu^a, \quad s\Omega_\mu^a = 0. \quad (2.18)$$

Finally, in order to control the dependence of the Green's functions on the background fields, we modify the STI functional of Eq.(2.16) as [34, 37]

$$\mathcal{S}'(\mathbb{I}')[\Phi, \Phi^*] = \mathcal{S}(\mathbb{I}')[\Phi, \Phi^*] + \Omega_\mu^a \left(\frac{\delta \mathbb{I}'}{\delta \widehat{A}_\mu^a} - \frac{\delta \mathbb{I}'}{\delta A_\mu^a} \right), \quad (2.19)$$

where \mathbb{I}' denotes the effective action that depends on the background sources Ω_μ^a , and $\mathcal{S}(\mathbb{I}')[\Phi, \Phi^*]$ is the STI functional of Eq.(2.16). Differentiation of the STI functional Eq.(2.19) with respect to the background source and background or quantum fields, will then relate 1PI functions involving background fields with the ones involving quantum fields (see Section III B below).

The final ingredient we need to know for the actual computation of STIs are the coupling of the anti-fields and background sources to the other fields of the theory. These are controlled by the Lagrangians

$$\begin{aligned} \mathcal{L}_{\text{BRST}} &= A_\mu^{*,a} \left[\partial_\mu c^a - g f^{abc} \left(A_\mu^b + \widehat{A}_\mu^b \right) c^c \right] - \frac{1}{2} g f^{abc} c^{*,a} c^b c^c + i g (\bar{\psi}^* c^a T^a \psi) + \text{h.c.}, \\ \mathcal{L}_\Omega &= \Omega_\mu^a \left[\partial_\mu \bar{c}^a - g f^{abc} \left(A_\mu^b + \widehat{A}_\mu^b \right) \bar{c}^c \right], \end{aligned} \quad (2.20)$$

from which the necessary Feynman rules can be derived. Notice that the Feynman rules for the vertices involving the background sources Ω^a are the same as the ones involving the anti-fields $A^{*,a}$ provided that we trade the ghost fields for anti-ghost fields.

III. THE BASIC INGREDIENTS

After having reviewed the BV formalism as it applies to the case of mass-less Yang-Mills theories, we next proceed to derive the basic ingredients needed for the PT construction. In particular we will focus on two aspects: (i) the derivation of the STI for the off-shell three-gluon vertex $\mathbb{I}_{A_\alpha A_\mu A_\beta}(q_1, q_2, q_3)$; as we will see this STI is of central importance for the intrinsic PT method, to be presented in Section VI. Of course the aforementioned STI is known since a long-time in the context of the standard formulation of non-Abelian gauge theories following the Faddeev-Popov Ansatz [25, 30]; here however we want to relate

in a *manifest* way the pieces appearing in it (ghost Green's functions) with well-defined quantities emerging in the BV formalism, *i.e.* auxiliary (unphysical) Green's functions involving ghost fields and gauge bosons anti-fields. (ii) the derivation of the BQIs relating the background and quantum two- three- and four-point functions. These identities furnish non-linear relations between the two kinds of Green's functions and facilitate significantly the eventual comparison between the effective PT Green's functions and the BFM Green's functions, computed at $\xi_Q = 1$. The crucial point is that the conventional Green's functions are related to the BFM ones by means of the same type of building blocks as those that appear in the STI of the three-gluon vertex, derived in (i), namely auxiliary, unphysical Green's functions. Even though the set of such auxiliary Green's functions appearing in (i) is different from that appearing in (ii), since the former involves ghost fields and gauge boson anti-fields, whereas the latter gauge boson background sources and anti-fields, it turns out that the two sets are related by a rather simple Schwinger-Dyson-type of relation, which we present here for the first time, in Eq.(3.23). This relation constitutes a non-trivial ingredient, bound to play a central role in the generalization of the intrinsic PT to all orders [26], and constitutes a central result of this section.

A. Slavnov-Taylor Identity for the three-gluon vertex

The standard text-book derivation of the three-gluon vertex STI starts from the trivial identity [30]

$$\langle 0|T [A_\mu^m(x)\bar{c}^b(y)[\partial^\nu A_\nu^c(z)]] |0\rangle = 0, \quad (3.1)$$

which is re-expressed in terms of the BRST-transformed fields, making also use of the equal-time commutation relation of the fields. The quantity which appears naturally when following this procedure and Fourier-transforming the identity into momentum space, is (from now on we assume that all momenta appearing in a given Green's function are entering, *i.e.*, $q_1 + q_2 + q_3 = 0$ in the case at hands)

$$L_{\alpha\beta}^{abc}(q_1, q_2, q_3) \equiv \int d^4x d^4y e^{-iq_1x} e^{-iq_3y} f^{aem} \langle 0|T [A_\alpha^e(x)c^m(x)\bar{c}^c(y)A_\beta^b(0)] |0\rangle, \quad (3.2)$$

which is written in the form

$$L_{\alpha\beta}^{abc}(q_1, q_2, q_3) \equiv \left[H_{\alpha\beta'}^{b'c'a}(q_2, q_3, q_1) + \Sigma_\alpha^{ad}(q_1) D^{de}(q_1) G_{\beta'}^{b'c'e}(q_2, q_3, q_1) \right] D^{cc'}(q_3) \Delta_\beta^{b'b\beta'}(q_2), \quad (3.3)$$

where we define the (full) ghost and gluon propagators (in the Feynman gauge) as follows

$$\begin{aligned}
D(p) &= \frac{i}{p^2 - iL(p)}, \\
\Delta_{\mu\nu}(q) &= -i \left[\Delta(q^2) P_{\mu\nu}(q) + \frac{q_\mu q_\nu}{q^4} \right], \quad \Delta(q^2) = \frac{1}{q^2 + i\Pi(q^2)}, \\
\Delta_{\mu\nu}^{(0)}(q) &= g_{\mu\nu} d(q), \quad d(q) = -iq^{-2}.
\end{aligned} \tag{3.4}$$

The scalar quantities $L(p)$ and $\Pi(q^2)$ represent respectively the ghost and gluon self-energies. The functions $\Sigma_\alpha^{ad}(q_1)$ and $G_{\beta'c'e}^{b'c'e}(q_2, q_3, q_1)$ are defined by means of the quantities

$$\begin{aligned}
N_\mu^{ab}(p) &\equiv \int d^4x e^{-ipx} f^{amn} \langle 0 | T [A_\mu^m(x) c^n(x) \bar{c}^b(0)] | 0 \rangle, \\
M_\mu^{abc}(q_1, q_2, q_3) &\equiv \int d^4x d^4y e^{-iq_3x} e^{-iq_2y} \langle 0 | T [c^c(x) \bar{c}^b(y) A_\mu^a(0)] | 0 \rangle,
\end{aligned} \tag{3.5}$$

as follows:

$$\begin{aligned}
gN_\mu^{ab}(p) &\equiv -\Sigma_\mu^{ac}(p) D^{cb}(p), \\
M_\mu^{abc}(q_1, q_2, q_3) &\equiv gG_{a'b'c'}^{\mu'}(q_1, q_2, q_3) \Delta_{\mu'\mu}^{a'a}(q_1) D^{b'b}(q_2) D^{c'c}(q_3).
\end{aligned} \tag{3.6}$$

Notice that (after eliminating the dependence on one momentum, using the constraint due to momentum conservation) the Green's functions H and Σ have the following diagrammatic definition

$$\begin{aligned}
H_{\alpha\beta}^{(n)}(q_1, q_2) &= \text{Diagram: A loop with three vertices. Top vertex is a circle labeled } \Delta_{\mu\nu}^{(n_2)}. \text{ Bottom vertex is a circle labeled } D^{(n_1)}. \text{ Right vertex is a circle labeled } \mathcal{K}_{\nu\beta}^{(n_3)}. \text{ Incoming wavy line from top-left is labeled } q_{1\alpha}. \text{ Incoming wavy line from top-right is labeled } q_{2\beta}. \text{ Outgoing dashed line from right vertex is labeled } \beta. \\
&\quad n = n_1 + n_2 + n_3 + 1 \\
&\quad n_1, n_2 \geq 0 \Leftrightarrow n_3 \geq 1 \\
&\quad \mathcal{K}_{\nu\beta}^{(0)} = \text{Diagram: A vertex with an incoming wavy line labeled } \nu \text{ and an outgoing dashed line labeled } \beta. \\
\\
\Sigma_\alpha^{(n)}(q_1) &= \text{Diagram: A loop with two vertices. Top vertex is a circle labeled } \Delta_{\mu\nu}^{(n_2)}. \text{ Bottom vertex is a circle labeled } D^{(n_1)}. \text{ Right vertex is a circle labeled } G_\nu^{(n_3)}. \text{ Incoming wavy line from top-left is labeled } q_{1\alpha}. \text{ Outgoing dashed line from right vertex is labeled } \alpha. \\
&\quad n = n_1 + n_2 + n_3 + 1
\end{aligned} \tag{3.7}$$

which at tree-level implies [30]

$$H_{\alpha\beta}^{(0)}(q_1, q_2) = \text{Diagram: A loop with two vertices. Top vertex is a circle labeled } \Delta_{\mu\nu}^{(0)}. \text{ Bottom vertex is a circle labeled } D^{(0)}. \text{ Incoming wavy line from top-left is labeled } q_{1\alpha}. \text{ Incoming wavy line from top-right is labeled } q_{2\beta}. \text{ Outgoing dashed line from bottom vertex is labeled } \alpha. \\
= -igg_{\alpha\beta} \tag{3.8}$$

Clearly, by definition in Eq.(3.3), $H_{\alpha\beta}(q_1, q_2)$ corresponds the one-particle irreducible part of $L_{\alpha\beta}(q_1, q_2)$, *i.e.*, graphically

$$L_{\alpha\beta}(q_1, q_2) = \text{Diagram 1} + \text{Diagram 2} \quad (3.9)$$

Notice the constraint on the values of n_1 , n_2 , and n_3 , appearing in the definition of $H_{\alpha\beta}^{(n)}(q_1, q_2)$. Clearly, since $H_{\alpha\beta}^{(n)}(q_1, q_2)$ corresponds to an *amputated* vertex, n_1 and n_2 may differ from zero, only iff $n_3 \geq 1$.

After standard manipulations one arrives at the well-known STI [25]

$$\begin{aligned} q_3^\nu \mathbb{I}_{A_\alpha A_\mu A_\nu}(q_1, q_2, q_3) &= [i\Delta_\alpha^{(-1)\rho}(q_1) + q_1^\rho q_{1\alpha}] [q_3^2 D(q_3)] H_{\rho\mu}(q_1, q_2) \\ &\quad - [i\Delta_\mu^{(-1)\rho}(q_2) + q_2^\rho q_{2\mu}] [q_3^2 D(q_3)] H_{\rho\alpha}(q_2, q_1), \end{aligned} \quad (3.10)$$

which, at tree-level, assumes the simple form

$$q_3^\nu \mathbb{I}_{A_\alpha A_\mu A_\nu}^{(0)}(q_1, q_2, q_3) = g [g_{\alpha\mu} q_2^2 - q_{2\alpha} q_{2\mu}] - g [g_{\alpha\mu} q_1^2 - q_{1\alpha} q_{1\mu}]. \quad (3.11)$$

In the BV formalism, the corresponding STI satisfied by the three-gluon vertex $\mathbb{I}_{A_\alpha^a A_\mu^b A_\nu^c}(q_1, q_2)$ may be obtained by considering the following functional differentiation of the STI functional of Eq.(2.16):

$$\left. \frac{\delta^3 \mathcal{S}(\mathbb{I})}{\delta c^c(q_3) \delta A_\mu^b(q_2) \delta A_\alpha^a(q_1)} \right|_{\Phi=0} = 0 \quad q_1 + q_2 + q_3 = 0, \quad (3.12)$$

which in turn gives the STI

$$\begin{aligned} &\mathbb{I}_{c^c A_\nu^{*,d}(-q_3) A_\mu^b A_\alpha^a}(q_2, q_1) + \mathbb{I}_{c^c A_\nu^{*,d} A_\mu^b A_\alpha^a}(q_2, q_1) \mathbb{I}_{A^{d,\nu} A_\mu^b}(q_2) \\ &+ \mathbb{I}_{c^c A_\nu^{*,d} A_\mu^b}(q_1, q_2) \mathbb{I}_{A^{d,\nu} A_\alpha^a}(q_1) = 0. \end{aligned} \quad (3.13)$$

We can then establish the following identifications [recall Eq.(2.17)]

$$\mathbb{I}_{A_\mu^a A_\nu^b}(q) = \delta^{ab} [iq_\mu q_\nu - \Delta_{\mu\nu}^{(-1)}(q)] \quad \Longrightarrow \quad \begin{cases} \mathbb{I}_{A_\mu A_\nu}^{(0)}(q) = -iq^2 P_{\mu\nu}(q), \\ \mathbb{I}_{A_\mu A_\nu}^{(n)}(q) = \Pi_{\mu\nu}^{(n)}(q^2). \end{cases} \quad (3.14)$$

Moreover we can factor out the Lorentz and group structure of the two-point function $\mathbb{I}_{c^a A_\mu^{*,b}}(p)$ appearing in Eq.(3.13) to get

$$\mathbb{I}_{c^a A_\mu^{*,b}}(p) = -i\delta^{ab} p_\mu \mathbb{I}_{cA^*}(p) \quad \Longrightarrow \quad \mathbb{I}_{cA^*}(p) = i \frac{p^\mu}{p^2} \mathbb{I}_{cA_\mu^*}(p). \quad (3.15)$$

It is then easy to show that the scalar quantity $\mathbb{I}_{cA}(p)$ is related to the ghost propagator by the following equation

$$\mathbb{I}_{cA^*}(p) = - [p^2 D(p)]^{(-1)}. \quad (3.16)$$

Using the Feynman rules derived from $\mathcal{L}_{\text{BRST}}$ (see Fig.1) to factor out the color structure function, we find

$$q_3^\nu \mathbb{I}_{A_\alpha A_\nu A_\mu}(q_1, q_2) \mathbb{I}_{cA^*}(q_3) = i \mathbb{I}_{cA_\rho^* A_\alpha}(q_2, q_1) \mathbb{I}_{A^\rho A_\mu}(q_2) - i \mathbb{I}_{cA_\rho^* A_\mu}(q_1, q_2) \mathbb{I}_{A^\rho A_\alpha}(q_1), \quad (3.17)$$

which implies the STI of Eq.(3.10), after the following identification

$$\mathbb{I}_{cA_\alpha^* A_\beta}(q_1, q_2) \equiv H_{\alpha\beta}(q_1, q_2). \quad (3.18)$$

This last relation will be helpful in making contact between the quantities appearing in the conventional STI formulated in the standard covariant gauges (which, as such, have no a-priori knowledge of the BV formalism) and quantities appearing in the BQI derived within the BV scheme.

B. Background-Quantum Identities

The BQIs were first presented in [33, 34] in the context of the Standard Model; they may be derived by appropriate functional differentiation of the BFM STI functional of Eq.(2.19) [38] .

1. Gluon two-point function

Consider the following functional differentiation of the STI functional Eq.(2.16)

$$\begin{aligned} \left. \frac{\delta^2 \mathcal{S}(\mathbb{I})}{\delta \Omega_\alpha^a(p_1) \delta \widehat{A}_\beta^b(q)} \right|_{\Phi=0} &= 0 & q + p_1 = 0, \\ \left. \frac{\delta^2 \mathcal{S}(\mathbb{I})}{\delta \Omega_\alpha^a(p_1) \delta A_\beta^b(q)} \right|_{\Phi=0} &= 0 & q + p_1 = 0, \end{aligned} \quad (3.19)$$

which will give the BQIs

$$\mathbb{I}_{\widehat{A}_\alpha^a \widehat{A}_\beta^b}(q) = \left[g_{\alpha\rho} \delta^{ad} + \mathbb{I}_{\Omega_\alpha^a A_\rho^{*,d}}(-p_1) \right] \mathbb{I}_{A^{d,\rho} \widehat{A}_\beta^b}(q), \quad (3.20)$$

$$\mathbb{I}_{\widehat{A}_\alpha^a A_\beta^b}(q) = \left[g_{\alpha\rho} \delta^{ad} + \mathbb{I}_{\Omega_\alpha^a A_\rho^{*,d}}(-p_1) \right] \mathbb{I}_{A^{d,\rho} A_\beta^b}(q). \quad (3.21)$$

$$\begin{array}{c} \text{Diagram 1: } \overline{\overline{A_\alpha^{*,a}}} \text{ (double line)} \rightarrow \text{wavy line } A_\beta^b \text{ and dashed line } c^c \text{ with value } -igf^{abc}g_{\alpha\beta} \\ \text{Diagram 2: } \overline{\overline{\Omega_\alpha^a}} \text{ (double line)} \rightarrow \text{wavy line } A_\beta^b \text{ and dashed line } c^c \text{ with value } -igf^{abc}g_{\alpha\beta} \end{array}$$

FIG. 1: Feynman rules from which the two- and three-point functions $\mathbb{I}_{\Omega_\alpha A_\beta^*}^{(n)}(q_1)$ and $\mathbb{I}_{cA_\alpha^* A_\beta}^{(n)}(q_1, q_2)$ can be built up.

We can now combine Eqs.(3.20) and (3.21) in such a way that the two-point function mixing background and quantum fields drops out [34]. Factoring out the gauge group invariant tensor δ^{ab} and the Lorentz transverse projector $P_{\alpha\beta}(q)$, we then arrive to the equation

$$\mathbb{I}_{\hat{A}\hat{A}}(q) = [1 + \mathbb{I}_{\Omega A^*}(q)]^2 \mathbb{I}_{AA}(q). \quad (3.22)$$

The quantity $\mathbb{I}_{\Omega A^*}(q)$ may be constructed order-by order using the Feynman rules derived from $\mathcal{L}_{\text{BRST}}$, listed in Fig.1.

The crucial point, which allows the exploitation of the BQIs derived above, is the observation that $\mathbb{I}_{\Omega A^*}(q)$ may be written in terms of the amplitudes D , Δ , and most importantly H , which appear in the STI for the three-gluon vertex, and are defined in the context of the conventional formalism, *i.e.*, have no a-priori knowledge of anti-fields, or of the Feynman rules stemming from $\mathcal{L}_{\text{BRST}}$.

In particular we have that the following Schwinger-Dyson equation holds (perturbatively)

$$i\mathbb{I}_{\Omega_\alpha A_\mu^*}^{(n)}(q) = C_A \int \frac{d^4 k}{(2\pi)^4} \mathbb{I}_{c\Omega_\alpha A_\mu}^{(0)}(q, -k - q) D^{(n_1)}(k) \Delta^{(n_2)\mu\nu}(k + q) \mathbb{I}_{cA_\beta^* A_\nu}^{(n_3)}(-q, k + q), \quad (3.23)$$

or diagrammatically

$$i\mathbb{I}_{\Omega_\alpha A_\beta^*}^{(n)}(q) = \text{Diagram} \quad n = n_1 + n_2 + n_3 + 1 \quad (3.24)$$

Clearly, from the basic Feynman rules of $\mathcal{L}_{\text{BRST}}$, we have that $\mathbb{I}_{cA_\alpha^* A_\beta}^{(0)}(q_1, q_2) = \mathbb{I}_{c\Omega_\alpha A_\beta}^{(0)}(q_1, q_2)$. Then using Eq.(3.18) we find

$$i\mathbb{I}_{\Omega_\alpha A_\beta^*}^{(n)}(q) = C_A \int \frac{d^4 k}{(2\pi)^4} H_{\alpha\mu}^{(0)}(q, -k - q) D^{(n_1)}(k) \Delta^{(n_2)\mu\nu}(k + q) H_{\beta\nu}^{(n_3)}(-q, k + q), \quad (3.25)$$

or, diagrammatically,

$$i\Pi_{\Omega_\alpha A_\beta^*}^{(n)}(q) = \text{Diagram} \quad n = n_1 + n_2 + n_3 + 1 \quad (3.26)$$

Evidently this last equation expresses $\Pi_{\Omega_\alpha A_\beta^*}^{(n)}(q)$, a quantity definable in the BV framework, entirely in terms of quantities definable in the conventional formalism. Using the diagrammatic definition of $H_{\alpha\mu}(q_1, q_2)$ shown in Eq.(3.7), we may express diagrammatically this last Schwinger-Dyson equation in terms of the four-particle kernel $\mathcal{K}_{\nu\rho}$ as follows,

$$i\Pi_{\Omega_\alpha A_\beta^*}^{(n)}(q) = \text{Diagram} \quad (3.27)$$

2. Gluon-quark-anti-quark three-point function

For the annihilation channel (one can study equally well the elastic channel) we consider the functional differentiation

$$\left. \frac{\delta^3 \mathcal{S}(\Pi)}{\delta \Omega_\alpha^a(q) \delta \bar{\psi}(Q') \delta \psi(Q)} \right|_{\Phi=0} = 0 \quad Q' + Q + q = 0, \quad (3.28)$$

which provides us the BQI

$$\begin{aligned} \Pi_{\hat{A}_\alpha^a \bar{\psi} \psi}(Q', Q) &= \left[g_{\alpha\rho} \delta^{ad} + \Pi_{\Omega_\alpha^a A_\rho^{*,d}}(-q) \right] \Pi_{A^{d,\rho} \bar{\psi} \psi}(Q', Q) + \Pi_{\bar{\psi} \psi}(-Q') \Pi_{\Omega_\alpha^a \bar{\psi}^* \psi}(Q', Q) \\ &- \Pi_{\Omega_\alpha^a \psi^* \bar{\psi}}(Q, Q') \Pi_{\bar{\psi} \psi}(Q). \end{aligned} \quad (3.29)$$

Since we will always deal with on-shell external fermions, we can sandwich the above equation between on-shell Dirac spinors; in this way, using the Dirac equations of motion $\Pi_{\bar{\psi} \psi}(Q) u(Q) = 0$ and $\bar{v}(Q') \Pi_{\bar{\psi} \psi}(-Q') = 0$ when $Q = Q' = m$, we can get rid of the second and third term appearing in Eq.(3.29), to write the on-shell BQI

$$\Pi_{\hat{A}_\alpha^a \bar{\psi} \psi}(Q', Q) = \left[g_{\alpha\rho} \delta^{ad} + \Pi_{\Omega_\alpha^a A_\rho^{*,d}}(q) \right] \Pi_{A^{d,\rho} \bar{\psi} \psi}(Q', Q). \quad (3.30)$$

The reader should appreciate the fact that the BQIs alone, interesting as they may be in their own right, would be of limited usefulness for our purposes, if it were not for the

complementary identification of the corresponding pieces appearing in the STI, as captured in Eq.(3.23). Notice in particular that the BQIs by themselves only amount to the statement that $\Gamma^{(n_1)}\Delta^{(n_2)}\Gamma^{(n_3)} = \widehat{\Gamma}^{(n_1)}\widehat{\Delta}^{(n_2)}\widehat{\Gamma}^{(n_3)}$, which is automatically true, since the box-diagrams are identical in both schemes, and so is the entire S -matrix.

3. Gluon three-point function

Here we derive the BQI relating the gluon three-point function $\mathbb{I}_{\widehat{A}_\alpha^a A_\beta^b A_\gamma^c}(p_1, p_2)$, *i.e.*, with one background and two quantum gluons to the normal gluon three-point function $\mathbb{I}_{A_\alpha^a A_\beta^b A_\gamma^c}(p_1, p_2)$ *i.e.*, with three quantum gluons.

We start by considering the following functional differentiation

$$\left. \frac{\delta^3 \mathcal{S}(\mathbb{I})}{\delta \Omega_\alpha^a(q) \delta A_\beta^b(p_1) \delta A_\gamma^c(p_2)} \right|_{\Phi=0} = 0 \quad q + p_1 + p_2 = 0, \quad (3.31)$$

which will provide us the BQI

$$\begin{aligned} \mathbb{I}_{\widehat{A}_\alpha^a A_\beta^b A_\gamma^c}(p_1, p_2) &= \left[g_{\alpha\rho} \delta^{ad} + \mathbb{I}_{\Omega_\alpha^a A_\rho^{*,d}}(q) \right] \mathbb{I}_{A^{d,\rho} A_\beta^b A_\gamma^c}(p_1, p_2) \\ &+ \mathbb{I}_{\Omega_\alpha^a A_\rho^{*,d} A_\gamma^c}(p_1, p_2) \mathbb{I}_{A^{d,\rho} A_\beta^b}(p_1) + \mathbb{I}_{\Omega_\alpha^a A_\rho^{*,d} A_\beta^b}(p_2, p_1) \mathbb{I}_{A^{d,\rho} A_\gamma^c}(p_2). \end{aligned} \quad (3.32)$$

Next, we consider the case in which the external gluons $A_\beta^b(p_1)$ and $A_\gamma^c(p_2)$ are “on-shell” physical states, *i.e.*, with $p_1^2 = p_2^2 = 0$ and $p_1^\beta \epsilon_\beta(p_1) = p_2^\gamma \epsilon_\gamma(p_2) = 0$. Then, since the gluon propagator is transverse, we find the on-shell BQI

$$\mathbb{I}_{\widehat{A}_\alpha^a A_\beta^b A_\gamma^c}(p_1, p_2) = \left[g_{\alpha\rho} \delta^{ad} + \mathbb{I}_{\Omega_\alpha^a A_\rho^{*,d}}(q) \right] \mathbb{I}_{A^{d,\rho} A_\beta^b A_\gamma^c}(p_1, p_2). \quad (3.33)$$

Notice that in the above BQI the (unphysical) Green’s function that provides the organization of the Feynman diagrams for converting the three-point function $\mathbb{I}_{\widehat{A}_\alpha^a A_\beta^b A_\gamma^c}(p_1, p_2)$ into the corresponding quantum one $\mathbb{I}_{A_\alpha^a A_\beta^b A_\gamma^c}(p_1, p_2)$, is the same that appears in the two-point BQI of Eqs.(3.22) and (3.30).

4. Gluon four-point function

Finally, we derive the BQI relating the gluon four-point function $\mathbb{I}_{\widehat{A}_\alpha^a A_\beta^b A_\gamma^c A_\delta^d}(p_1, p_2, p_3)$, *i.e.*, with one background and three quantum gluons to the normal gluon four-point function $\mathbb{I}_{A_\alpha^a A_\beta^b A_\gamma^c A_\delta^d}(p_1, p_2, p_3)$, *i.e.*, with four quantum gluons.

For doing this we consider the functional differentiation

$$\left. \frac{\delta^4 \mathcal{S}(\mathbb{I})}{\delta \Omega_\alpha^a(q) \delta A_\beta^b(p_1) \delta A_\gamma^c(p_2) \delta A_\delta^d(p_3)} \right|_{\Phi=0} = 0 \quad q + p_1 + p_2 + p_3 = 0, \quad (3.34)$$

which will give us the BQI

$$\begin{aligned} \mathbb{I}_{\hat{A}_\alpha^a A_\beta^b A_\gamma^c A_\delta^d}(p_1, p_2, p_3) &= \left[g_{\alpha\rho} \delta^{ae} + \mathbb{I}_{\Omega_\alpha^a A_\rho^{*,e}}(q) \right] \mathbb{I}_{A^{e,\rho} A_\beta^b A_\gamma^c A_\delta^d}(p_1, p_2, p_3) \\ &+ \mathbb{I}_{\Omega_\alpha^a A_\rho^{*,e} A_\beta^b}(q, p_1) \mathbb{I}_{A^{e,\rho} A_\gamma^c A_\delta^d}(q + p_1, p_2) \\ &+ \mathbb{I}_{\Omega_\alpha^a A_\rho^{*,e} A_\gamma^c}(q, p_2) \mathbb{I}_{A^{e,\rho} A_\delta^d A_\beta^b}(q + p_2, p_3) \\ &+ \mathbb{I}_{\Omega_\alpha^a A_\rho^{*,e} A_\delta^d}(q, p_3) \mathbb{I}_{A^{d,\rho} A_\beta^b A_\gamma^c}(q + p_3, p_1) \\ &+ \mathbb{I}_{\Omega_\alpha^a A_\beta^b A_\gamma^c A_\rho^{*,e}}(q, p_1, p_2) \mathbb{I}_{A^{e,\rho} A_\delta^d}(p_3) \\ &+ \mathbb{I}_{\Omega_\alpha^a A_\delta^d A_\beta^b A_\rho^{*,e}}(q, p_3, p_1) \mathbb{I}_{A^{e,\rho} A_\gamma^c}(p_2) \\ &+ \mathbb{I}_{\Omega_\alpha^a A_\gamma^c A_\delta^d A_\rho^{*,e}}(q, p_2, p_3) \mathbb{I}_{A^{e,\rho} A_\beta^b}(p_1). \end{aligned} \quad (3.35)$$

If, as before, the external gluons $A_\beta^b(p_1)$, $A_\gamma^c(p_2)$ and $A_\delta^d(p_3)$ are considered as on-shell physical states, we can get rid of the last three terms, obtaining the on-shell BQI

$$\begin{aligned} \mathbb{I}_{\hat{A}_\alpha^a A_\beta^b A_\gamma^c A_\delta^d}(p_1, p_2, p_3) &= \left[g_{\alpha\rho} \delta^{ae} + \mathbb{I}_{\Omega_\alpha^a A_\rho^{*,e}}(q) \right] \mathbb{I}_{A^{e,\rho} A_\beta^b A_\gamma^c A_\delta^d}(p_1, p_2, p_3) \\ &+ \mathbb{I}_{\Omega_\alpha^a A_\rho^{*,e} A_\beta^b}(q, p_1) \mathbb{I}_{A^{e,\rho} A_\gamma^c A_\delta^d}(q + p_1, p_2) \\ &+ \mathbb{I}_{\Omega_\alpha^a A_\rho^{*,e} A_\gamma^c}(q, p_2) \mathbb{I}_{A^{e,\rho} A_\delta^d A_\beta^b}(q + p_2, p_3) \\ &+ \mathbb{I}_{\Omega_\alpha^a A_\rho^{*,e} A_\delta^d}(q, p_3) \mathbb{I}_{A^{d,\rho} A_\beta^b A_\gamma^c}(q + p_3, p_1). \end{aligned} \quad (3.36)$$

Again we find the same unphysical Green's function emerging, plus three terms that were not present (due to the on-shell condition) in Eq.(3.33).

IV. A FRESH LOOK AT THE S -MATRIX PT

In the next two sections we will review the S -matrix PT in an attempt to accomplish two main objectives. First, we will furnish a discussion of the method, which incorporates into a coherent framework the various conceptual and technical development which have taken place in the last years. Second, we use it as an opportunity to familiarize ourselves with the BV formalism, and in particular the BQIs, in a well-understood context. Thus, after outlining the general PT framework, we will re-express the one-loop S -matrix PT results in terms of the BV building blocks. The more technical case of the two-loop PT, together with the corresponding BV ingredients, will be revisited in the next section.

A. General framework

A general S -matrix element of a $2 \rightarrow 2$ process can be written following the standard Feynman rules as

$$T(s, t, m_i) = T_1(s, \xi) + T_2(s, m_i, \xi) + T_3(s, t, m_i, \xi), \quad (4.1)$$

Evidently the Feynman diagrams impose a decomposition of $T(s, t, m_i)$ into three distinct sub-amplitudes T_1 , T_2 , and T_3 , with a very characteristic kinematic structure, *i.e.*, a very particular dependence on the the Mandelstam kinematic variables and the masses. Thus, T_1 is the conventional self-energy contribution, which only depends on the momentum transfer s , T_2 corresponds to vertex diagrams which in general depend also on the masses of the external particles, whereas T_3 is a box-contribution, having in addition a non-trivial dependence on the Mandelstam variable t . However, all these sub-amplitudes, in addition to their dependence of the physical kinematic variables, also display a non-trivial dependence on the unphysical gauge fixing parameter parameter ξ . Of course we know that the BRST symmetry guarantees that the total $T(s, t, m_i)$ is independent of ξ , *i.e.*, $dT/d\xi = 0$; thus, in general, a set of delicate gauge-cancellations will take place. The PT framework provides a very particular realization of this cancellations. Specifically, the transition amplitude $T(s, t, m_i)$ of a $2 \rightarrow 2$ process, can be decomposed as [1, 2, 3]

$$T(s, t, m_i) = \hat{T}_1(s) + \hat{T}_2(s, m_i) + \hat{T}_3(s, t, m_i), \quad (4.2)$$

in terms of three individually gauge-invariant quantities: a propagator-like part (\hat{T}_1), a vertex-like piece (\hat{T}_2), and a part containing box graphs (\hat{T}_3). The important observation is that vertex and box graphs contain in general pieces, which are kinematically akin to self-energy graphs of the transition amplitude. The PT is a systematic way of extracting such pieces and appending them to the conventional self-energy graphs. In the same way, effective gauge invariant vertices may be constructed, if after subtracting from the conventional vertices the propagator-like pinch parts we add the vertex-like pieces, if any, coming from boxes. The remaining purely box-like contributions are then also gauge invariant. In what follows we will consider for concreteness the S -matrix element for the quark (q)-antiquark (\bar{q}) elastic scattering process $q(P)\bar{q}(P') \rightarrow q(Q)\bar{q}(Q')$ in QCD; we set $q = P' - P = Q' - Q$, with $s = q^2$ is the square of the momentum transfer. One could equally well study the annihilation channel, in which case s would be the center-of-mass energy.

In order to identify the pieces which are to be reassigned, all one has to do is to resort to the fundamental WIs of the theory. In particular the longitudinal momenta k_μ appearing inside Feynman diagrams eventually reach the elementary gluon-quark vertex involving one “on-shell” quark carrying momentum Q and one off-shell quark, carrying momentum $k + Q$, and trigger the WI

$$\begin{aligned}
k_\mu [\bar{u}(Q) \gamma^\mu S(k + Q)] &= \bar{u}(Q) \not{k} S(k + Q) \\
&= \bar{u}(Q) [(k + Q + m) - (Q + m)] S(k + Q) \\
&= \bar{u}(Q) [S^{-1}(k + Q) - S^{-1}(Q)] S(k + Q)
\end{aligned} \tag{4.3}$$

The first term in the square bracket will remove (pinch out) the internal quark propagator, giving rise to a self-energy-like contributions, while the second term will die on-shell, by virtue of the Dirac equation of motion; the on-shell condition used at this point is characteristic of the S -matrix PT [1, 2, 3].

An important step in the PT procedure is clearly the identification of all *longitudinal* momenta involved, *i.e.*, the momenta which can trigger the elementary WI of Eq.(4.11). There are two sources of such momenta: (i) The tree-level expressions for the gauge boson propagators appearing inside Feynman diagrams and (ii) the tri-linear gauge boson vertices. Regarding the former contributions, the tree-level gluon propagator reads

$$\Delta_{\mu\nu}(q) = \frac{-i}{q^2} \left[g_{\mu\nu} - (1 - \xi) \frac{q_\mu q_\nu}{q^2} \right], \tag{4.4}$$

and the longitudinal momenta are simply those multiplying $(1 - \xi)$. It is a straightforward but tedious exercise to convince one-self that inside an S -matrix element all terms proportional to $(1 - \xi)^n$, with $n \geq 1$, cancel against each-other in a very special way. In particular, all relevant cancellations proceed without need of carrying out integrations over the virtual loop momenta, thus maintaining the kinematic identity of the various Green’s functions intact, a point of crucial importance within the PT philosophy. As has been shown by explicit calculations (see for example [39]), this is indeed the case at one- and two-loops. The key observation is that all contributions originating from the longitudinal parts of gauge boson propagators, by virtue of the WIs they trigger, give rise to *unphysical* effective vertices, *i.e.*, vertices which do not exist in the original Lagrangian. All such vertices cancel *diagrammatically* inside ostensibly gauge-invariant quantities, such as current correlation functions or S -matrix elements. It is important to emphasize that exactly the same result is

obtained even in the context of the non-covariant axial gauges (see for example [40, 41, 42]), where the Feynman gauge cannot be reached a priori by simply fixing appropriately the value of the gauge-fixing parameter. Thus, even if one uses a bare gluon propagator of the general axial gauge form, after the aforementioned cancellations have taken place one arrives effectively to the answer written in the covariant Feynman gauge. Thus, one can begin the analysis without loss of generality by choosing the Feynman gauge when writing down the Feynman diagrams contributing to the S -matrix.

The identification and role of the longitudinal momenta stemming from the three-gluon vertex is slightly more subtle. The fundamental tree-level three-gluon vertex $\Pi_{A_\alpha^a A_\mu^b A_\nu^c}^{(0)}(q, p_1, p_2)$ is given by the following manifestly Bose-symmetric expression (all momenta are incoming, *i.e.*, $q + p_1 + p_2 = 0$)

$$\begin{aligned}\Pi_{A_\alpha^a A_\mu^b A_\nu^c}^{(0)}(q, p_1, p_2) &= g f^{abc} \Gamma_{\alpha\mu\nu}^{(0)}(q, p_1, p_2), \\ \Gamma_{\alpha\mu\nu}^{(0)}(q, p_1, p_2) &= (q - p_1)_\nu g_{\alpha\mu} + (p_1 - p_2)_\alpha g_{\mu\nu} + (p_2 - q)_\mu g_{\alpha\nu}.\end{aligned}\quad (4.5)$$

The Lorentz structure $\Gamma_{\alpha\mu\nu}^{(0)}(q, p_1, p_2)$ may be split into two parts [43, 44]

$$\Gamma_{\alpha\mu\nu}^{(0)}(q, p_1, p_2) = \Gamma_{\alpha\mu\nu}^F(q, p_1, p_2) + \Gamma_{\alpha\mu\nu}^P(q, p_1, p_2), \quad (4.6)$$

with

$$\begin{aligned}\Gamma_{\alpha\mu\nu}^F(q, p_1, p_2) &= (p_1 - p_2)_\alpha g_{\mu\nu} + 2q_\nu g_{\alpha\mu} - 2q_\mu g_{\alpha\nu}, \\ \Gamma_{\alpha\mu\nu}^P(q, p_1, p_2) &= p_{2\nu} g_{\alpha\mu} - p_{1\mu} g_{\alpha\nu}.\end{aligned}\quad (4.7)$$

The vertex $\Gamma_{\alpha\mu\nu}^F(q, p_1, p_2)$ is Bose-symmetric only with respect to the μ and ν legs, and coincides with the BFM Feynman gauge bare vertex involving one background gluon (carrying four-momentum q) and two quantum gluons (carrying four-momenta p_1 and p_2). Evidently the above decomposition assigns a special rôle to the q -leg, and allows $\Gamma_{\alpha\mu\nu}^F(q, p_1, p_2)$ to satisfy the WI

$$q^\alpha \Gamma_{\alpha\mu\nu}^F(q, p_1, p_2) = (p_2^2 - p_1^2) g_{\mu\nu}, \quad (4.8)$$

where the right-hand side (RHS) is the difference of two-inverse propagators in the renormalizable Feynman gauge. The term $\Gamma_{\alpha\mu\nu}^P(q, p_1, p_2)$ contains the pinching momenta; they will eventually trigger the elementary WI, which will eliminate the internal quark propagator, resulting in an effectively propagator-like contribution. Notice that in the light of the BV

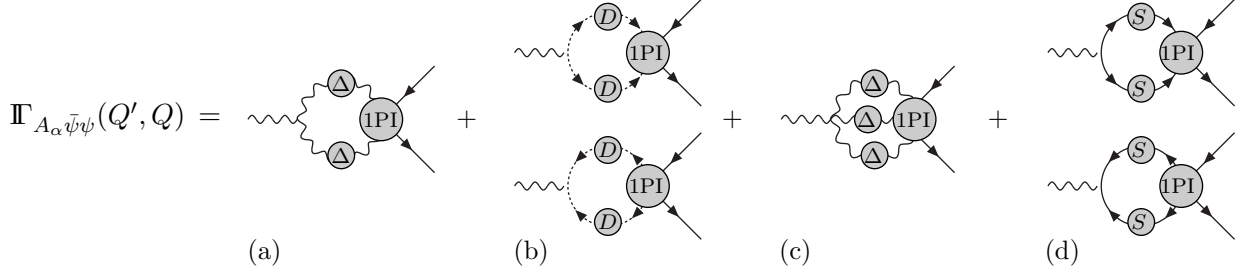


FIG. 2: The decomposition of the three-point function $\Pi_{A_\alpha \bar{\psi} \psi}(Q', Q)$ in terms of diagrams having an external elementary three-gluon vertex $\Gamma_{A_\alpha \bar{\psi} \psi}^{A^2}(Q', Q)$ (a), those where the external gluon couples directly to ghost fields $\Gamma_{A_\alpha \bar{\psi} \psi}^{\bar{c}c}(Q', Q)$ (b), and the the rest, which falls into neither of the previous categories $\Gamma_{A_\alpha \bar{\psi} \psi}^{A^3}(Q', Q)$ and $\Gamma_{A_\alpha \bar{\psi} \psi}^{\bar{q}q}(Q', Q)$ [(c) and (d) respectively]. S represents the full fermionic propagator.

formalism, the PT splitting given in Eq.(4.7) may be cast in the alternative, perhaps more suggestive form

$$\Pi_{A_\alpha A_\mu^b A_\nu^c}^{(0)}(q, p_1, p_2) = \Pi_{\hat{A}_\alpha A_\mu^b A_\nu^c}^{(0)}(q, p_1, p_2) + i \left[p_{2\nu} \Pi_{cA_\alpha^* A_\mu}^{(0)} - p_{1\mu} \Pi_{cA_\alpha^* A_\nu}^{(0)} \right]. \quad (4.9)$$

According to the PT [23, 24] the next steps consists of the following: (a) Classify all diagrams which contribute to the three-point function $\Pi_{A_\alpha \bar{\psi} \psi}(Q', Q)$ into the following categories: (i) those containing an *external* three-gluon vertex, *i.e.*, a three-gluon vertex where the momentum q is incoming, (ii) those which do not have such an external three-gluon vertex. This latter set contains graphs where the incoming gluon couples to the rest of the diagram with any type of interaction vertex other than a three-gluon vertex. Thus we write (see also Fig.2)

$$\Pi_{A_\alpha \bar{\psi} \psi}(Q', Q) = \Gamma_{A_\alpha \bar{\psi} \psi}^{A^2}(Q', Q) + \Gamma_{A_\alpha \bar{\psi} \psi}^{\bar{c}c}(Q', Q) + \Gamma_{A_\alpha \bar{\psi} \psi}^{A^3}(Q', Q) + \Gamma_{A_\alpha \bar{\psi} \psi}^{\bar{q}q}(Q', Q). \quad (4.10)$$

(b) Carry out inside the class (i) diagrams the vertex decomposition given in Eq.(4.6). (c) Track down the terms originating from $\Gamma_{\alpha\mu\nu}^P(q, p_1, p_2)$: these terms, depending on the topological details of the diagram under consideration will either (i) trigger directly the WI of Eq.(4.3) or (ii) they will trigger a chain of intermediate tree-level WIs, such as Eq.(6.1) whose end result will be that eventually an appropriate longitudinal momentum will be generated, which will trigger the WI of Eq.(4.3). (d) The propagator-like terms thusly generated are to be allotted to the conventional self-energy graphs, and will form part of the

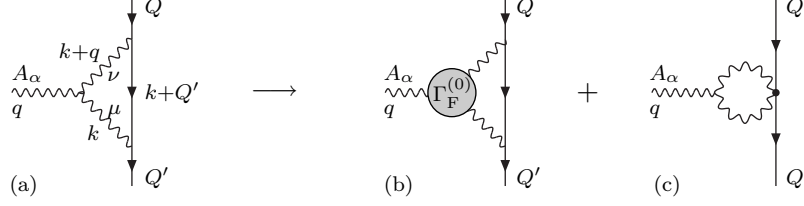


FIG. 3: Carrying out the fundamental vertex decomposition inside the three-point function $\Gamma_{A_\alpha\psi\bar{\psi}}^{A^2(1)}(Q', Q)$ (a) contributing to $\Pi_{A_\alpha\psi\bar{\psi}}^{(1)}(Q', Q)$, gives rise to the genuine vertex $\hat{\Gamma}_{A_\alpha\psi\bar{\psi}}^{A^2(1)}(Q', Q)$ (b) and a self-energy-like contribution $\frac{1}{2}V_{\alpha\rho}^P(q)\gamma^\rho$ (c).

effective PT gluon self-energy at that order; to complete its construction one needs to supply in addition the left-over pieces generated when converting a string of 1PI self-energies into a corresponding PT string. Finally, the remaining purely vertex-like parts define the effective PT gluon-quark-antiquark three-point function $\hat{\Pi}_{A_\alpha\bar{\psi}\psi}(Q', Q)$.

Before entering into some of the details of the explicit one- and two-loop constructions we would like to comment on an additional subtle point. One of the main obstacle related to the generalization of the PT beyond one-loop has been the issue of whether or not a splitting analogous to that of Eq.(4.6) should take place for the internal three-gluon vertices, *i.e.*, vertices with all three legs irrigated by virtual momenta, so that q never enters *alone* into any of the legs. This issue has been resolved by resorting to the special unitarity properties satisfied by the PT Green's functions. The final answer is that no splitting should take place for *any* of these internal three-gluon vertices. As we will see in the next section, a new and more direct argument corroborates this answer.

B. The one-loop construction

Notice that at the one-loop level only the first and last term of Eq.(4.10) will be present. We then implement (see Fig.3a) the vertex decomposition of Eq.(4.6), with $p_{1\mu} = k_\mu$, $p_{2\nu} = -(k+q)_\nu$, inside the $\Gamma_{A_\alpha\bar{\psi}\psi}^{A^2(1)}(Q', Q)$ part of Eq.(4.10). The $\Gamma_{\alpha\mu\nu}^P(q, p_1, p_2)$ term triggers then the elementary WIs

$$\begin{aligned} \not{k} &= (\not{k} + \not{Q}' - m) - (\not{Q}' - m), \\ \not{k} + \not{q} &= (\not{k} + \not{Q}' - m) - (\not{Q} - m), \end{aligned} \quad (4.11)$$

thus, two self-energy like pieces are generated (Fig.3c), which are to be allotted to the conventional self-energy. In particular,

$$\begin{aligned}\Gamma_{A_\alpha\bar{\psi}\psi}^{A^2(1)}(Q', Q) &= \widehat{\Gamma}_{A_\alpha\bar{\psi}\psi}^{A^2(1)}(Q', Q) + \frac{1}{2}V_{\alpha\rho}^{\text{P}(1)}(q)\gamma^\rho - X_{1\alpha}^{(1)}(Q', Q)\Sigma^{(0)}(Q') \\ &\quad - \Sigma^{(0)}(Q)X_{2\alpha}^{(1)}(Q', Q),\end{aligned}\tag{4.12}$$

where

$$\begin{aligned}\widehat{\Gamma}_{A_\alpha\bar{\psi}\psi}^{A^2(1)}(Q', Q) &= \int_{L_1} J(q, k)\Gamma_{\alpha\mu\nu}^{\text{F}}(q, k, -k - q)\gamma^\mu S^{(0)}(Q' + k)\gamma^\nu, \\ V_{\alpha\rho}^{\text{P}(1)}(q) &= 2g_{\alpha\rho} \int_{L_1} J(q, k),\end{aligned}\tag{4.13}$$

and

$$\begin{aligned}\int_{L_1} &\equiv \mu^{2\varepsilon} \int \frac{d^d k}{(2\pi)^d}, \\ J(q, k) &\equiv g^2 C_A [k^2(k + q)^2]^{-1}.\end{aligned}\tag{4.14}$$

C_A denotes the Casimir eigenvalue of the adjoint representation, *i.e.*, $C_A = N$ for $SU(N)$. Notice that the last two terms appearing in the RHS of Eq.(4.12) vanish for on-shell external fermions, and will be discarded in the analysis that follows.

The (dimension-less) self-energy-like contribution $\frac{1}{2}V_{\alpha\rho}^{\text{P}(1)}(q)$, together with another such contribution arising from the mirror vertex (not shown), after trivial manipulations gives rise to the dimensionful quantity

$$\begin{aligned}\Pi_{\alpha\beta}^{\text{P}(1)}(q) &= q^2 V_{\alpha\rho}^{\text{P}(1)}(q)P_\beta^\rho(q) = \Pi^{\text{P}(1)}(q)P_{\alpha\beta}(q), \\ \Pi^{\text{P}(1)}(q) &= 2q^2 \int_{L_1} J(q, k).\end{aligned}\tag{4.15}$$

$\Pi_{\alpha\beta}^{\text{P}(1)}(q)$ will be added to the conventional one-loop gluon two-point function $\Pi_{A_\alpha A_\beta}^{(1)}(q)$, to give rise to the the PT one-loop gluon two-point function $\widehat{\Pi}_{A_\alpha A_\beta}^{(1)}(q)$ (see Fig.4):

$$\widehat{\Pi}_{A_\alpha A_\beta}^{(1)}(q) = \Pi_{A_\alpha A_\beta}^{(1)}(q) + \Pi_{\alpha\beta}^{\text{P}(1)}(q).\tag{4.16}$$

Correspondingly, the PT one-loop three-point function $\widehat{\Pi}_{A_\alpha\bar{\psi}\psi}^{(1)}(Q', Q)$ will be defined as

$$\begin{aligned}\widehat{\Pi}_{A_\alpha\bar{\psi}\psi}^{(1)}(Q', Q) &= \widehat{\Gamma}_{A_\alpha\bar{\psi}\psi}^{A^2(1)}(Q', Q) + \Gamma_{A_\alpha\bar{\psi}\psi}^{\bar{q}q(1)} \\ &= \Pi_{A_\alpha\bar{\psi}\psi}^{(1)}(Q', Q) - \frac{1}{2}V_{\alpha\rho}^{\text{P}(1)}(q)\gamma^\rho.\end{aligned}\tag{4.17}$$

$$\widehat{\Pi}_{A_\alpha A_\beta}^{(1)}(q) = \frac{1}{2} \text{(a)} + \text{(b)} + 2 \text{(c)} P_{\alpha\beta}(q)$$

FIG. 4: The diagrammatic representation of the PT two-point function $\widehat{\Pi}_{A_\alpha A_\beta}^{(1)}(q)$ as the sum of the conventional two-point function $\Pi_{A_\alpha A_\beta}^{(1)}(q)$ given by (a) and (b), and the pinch contributions coming from the vertices (c).

We can then compare these results with the ones we can get from the BQIs of Eqs.(3.22) and (3.30) found in the previous sections. At one loop these BQIs read

$$\begin{aligned} \Pi_{\widehat{A}_\alpha \widehat{A}_\beta}^{(1)}(q) &= \Pi_{A_\alpha A_\beta}^{(1)}(q) + 2\Pi_{\Omega_\alpha A_\rho^*}^{(1)}(q)\Pi_{A^\rho A_\beta}^{(0)}(q), \\ \Pi_{\widehat{A}_\alpha \widehat{\bar{\psi}\psi}}^{(1)}(Q', Q) &= \Pi_{A_\alpha \bar{\psi}\psi}^{(1)}(Q', Q) + \Pi_{\Omega_\alpha A_\rho^*}^{(1)}(q)\Pi_{A^\rho \bar{\psi}\psi}^{(0)}(Q', Q), \end{aligned} \quad (4.18)$$

where in the last equation we factor out a gT^a factor.

From the perturbative expansion of Eq.(3.23), observing that $i\Pi_{\Omega_\mu^a A_\nu^{*,b}}^{(n)}(q) = \Pi_{\Omega_\mu^a A_\nu^{*,b}}^{(n)}(q)$, one has

$$i\Pi_{\Omega_\alpha^a A_\rho^{*,b}}^{(1)}(q) = \text{Diagram} = i\delta^{ab}\Pi_{\Omega_\alpha A_\rho^*}^{(1)}(q)$$

Therefore, using the Feynman rules of Fig.1, we find

$$\begin{aligned} \Pi_{\Omega_\alpha A_\rho^*}^{(1)}(q) &= ig_{\alpha\rho} \int_{L_1} J(q, k) \\ &= \frac{i}{2} V_{\alpha\rho}^{\text{P}(1)}(q). \end{aligned} \quad (4.19)$$

Thus one has the results

$$\begin{aligned} 2\Pi_{\Omega_\alpha A_\rho^*}^{(1)}(q)\Pi_{A^\rho A_\beta}^{(0)}(q) &= \Pi_{\alpha\beta}^{\text{P}(1)}(q), \\ \Pi_{\Omega_\alpha A_\rho^*}^{(1)}(q)\Pi_{A^\rho \bar{\psi}\psi}^{(0)}(Q', Q) &= -\frac{1}{2} V_{\alpha\rho}^{\text{P}(1)}(q)\gamma^\rho, \end{aligned}$$

which will in turn automatically enforce the identifications

$$\begin{aligned} \widehat{\Pi}_{A_\alpha A_\beta}^{(1)}(q) &\equiv \Pi_{\widehat{A}_\alpha \widehat{A}_\beta}^{(1)}(q), \\ \widehat{\Pi}_{A_\alpha \bar{\psi}\psi}^{(1)}(Q', Q) &\equiv \Pi_{\widehat{A}_\alpha \bar{\psi}\psi}^{(1)}(Q', Q). \end{aligned} \quad (4.20)$$

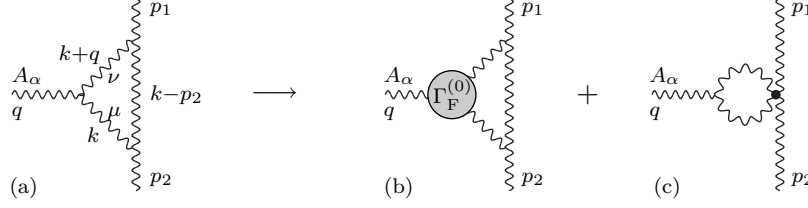


FIG. 5: The result of carrying out the PT decomposition on the three-point function $\Pi_{A_\alpha A_\beta A_\gamma}^{A^2(1)}(p_1, p_2)$ for the case of two external on-shell gluons. Notice that in graph (c), despite appearances, the vertex connecting the loop to the external gluons is a tree- and not a four-gluon vertex.

C. Universality (process-independence) of the PT algorithm

One important question has been whether the construction of off-shell Green's functions, such as an effective gluon self-energy, depends on the kind of external particles chosen. This question was settled in [45] by means of detailed calculations. In particular it has been shown that at one-loop the gluon self-energy constructed by resorting to the PT algorithm is universal, in the sense that it does not depend on the specific process where it is embedded. In this subsection we will show how one can arrive at this result with the aid of the BQIs appearing in Eqs.(3.33) and (3.36).

We will construct $\widehat{\Pi}_{A_\alpha A_\beta}^{(1)}(q)$ by considering the process $g_{\rho_1}^{c_1}(p_1)g_{\rho_2}^{c_2}(p_2) \rightarrow g_{\rho_3}^{c_3}(p_3)g_{\rho_4}^{c_4}(p_4)$, where the $g_{\rho_i}^{c_i}(p_i)$ represent on-shell gluons, *i.e.*, with $p_i^2 = 0$ and $p_i^{\rho_i}\epsilon_{\rho_i}(p_i) = 0$.

The PT algorithm in this case amounts to carrying out the characteristic three-gluon vertex decomposition of Eq.(4.6) to the graphs contributing to $\Pi_{A_\alpha A_{\rho_1}^{c_1} A_{\rho_2}^{c_2}}^{(1)}(q, p_1, p_2)$, which have an external three-gluon vertex; there are two such graphs, out of which only that of Fig.5a gives rise to a propagator-like contribution. In particular, the longitudinal momenta k_μ and $(k+q)_\nu$ appearing in $\Gamma_{\alpha\mu\nu}^P(q, k, -k-q)$ will be contracted with the corresponding three-gluon vertex where one of the two on-shell gluons is entering ($g_{\rho_1}^{c_1}(p_1)$ and $g_{\rho_2}^{c_2}(p_2)$, respectively) triggering the tree-level WI of Eq.(3.11), which is the exact analogue of Eq.(4.11) in the case when the external particles are gluons instead of quarks. It is straightforward to verify that again the internal gluon propagator of momentum $k-p_2$ will be canceled by the corresponding piece stemming from the WI of Eq.(3.11), giving rise to the propagator-like diagram of Fig.5c. This piece is simply given by (after the standard insertion of $d(q)d^{-1}(q)$)

and use of the on-shell conditions)

$$\Gamma_{\beta\rho_3\rho_4}^{(0)}(q, p_3, p_4) d(q) \left[\frac{1}{2} \Pi_{\beta\alpha}^{\text{P}(1)}(q) \right] d(q) \Gamma_{\alpha\rho_1\rho_2}^{(0)}(q, p_1, p_2). \quad (4.21)$$

After multiplication by a factor of 2 to take into account the mirror graphs (not shown) the above contribution is added to the usual propagator contributions, also sandwiched between $\Gamma_{\beta\rho_3\rho_4}^{(0)}(q, p_3, p_4)$ and $\Gamma_{\alpha\rho_1\rho_2}^{(0)}(q, p_1, p_2)$ to give rise to the $\hat{\Pi}_{A_\alpha A_\beta}^{(1)}(q)$ of Eq.(4.16). A straightforward algebraic manipulation of the remaining terms stemming from the WI shows that they either vanish on-shell, or they combine with the rest of the diagrams (not shown) to give rise precisely to the one-loop vertex $\Pi_{\hat{A}_\alpha A_{\rho_1}^{c_1} A_{\rho_2}^{c_2}}^{(1)}(q, p_1, p_2)$. Of course, in the light of Eq.(3.33) this is exactly what one should obtain, since the subtraction from $\Pi_{A_\alpha A_{\rho_1}^{c_1} A_{\rho_2}^{c_2}}^{(1)}(q, p_1, p_2)$ of the term given in Eq.(4.21), is nothing but $\Pi_{\hat{A}_\alpha A_{\rho_1}^{c_1} A_{\rho_2}^{c_2}}^{(1)}(q, p_1, p_2)$.

We next turn to the slightly more involved case of constructing $\hat{\Pi}_{A_\alpha A_\beta}^{(1)}(q)$ by embedding it in the process $g_{\rho_1}^{c_1}(p_1)g_{\rho_2}^{c_2}(p_2)g_{\rho_3}^{c_3}(p_3) \rightarrow g_{\rho_3}^{c_4}(p_4)g_{\rho_5}^{c_5}(p_5)g_{\rho_6}^{c_6}(p_6)$, where, as before, the $g_{\rho_i}^{c_i}(p_i)$ represent on-shell gluons, with $p_i^2 = 0$ and $p_i^{\rho_i}\epsilon_{\rho_i}(p_i) = 0$.

As before, one should carry out the characteristic three-gluon vertex decomposition of Eq.(4.6) to the graphs which have an external three-gluon vertex; there are various such graphs, but the essence of the relevant rearrangements can be captured by looking at the graphs shown in Fig.6. The graph of Fig.6a contributes to the 1PI one-loop four-gluon vertex $\Pi_{A_\alpha A_{\rho_1}^{c_1} A_{\rho_2}^{c_2} A_{\rho_3}^{c_3}}^{(1)}(q, p_1, p_2, p_3)$, whereas the graph of Fig.6e is 1PR and contributes to the one-loop three-gluon vertex nested inside the process we consider. Notice in particular that unlike the one-loop three-gluon vertex considered in the previous process (Fig.5a), the one appearing in Fig.6e has not one but two off-shell legs (those carrying momenta q and $p_1 + p_2$).

The action of the longitudinal (pinching) momenta stemming from the PT decomposition of the external tree-level three-gluon vertex appearing in the graph of Fig.6a gives rise to the propagator-like contribution of Fig.6c, given by the same expression as in Eq.(4.21), with the only difference that the contribution $d(q) \left[\frac{1}{2} \Pi_{\beta\alpha}^{\text{P}(1)}(q) \right] d(q)$ is sandwiched between two tree-level four-gluon vertices instead of two tree-level three-gluon vertices. In addition to this propagator-like contribution the pinching momenta give also rise to contributions of the type shown in Fig.6d, by virtue of the elementary WI

$$\begin{aligned} q_1^\mu \Pi_{A_\mu^a A_\nu^b A_\alpha^c A_\beta^d}^{(0)}(q_1, q_2, q_3, q_4) &= -f^{abe} \Pi_{A_\alpha^c A_\beta^d A_\nu^e}^{(0)}(q_3, q_4, q_1 + q_2) - f^{ace} \Pi_{A_\beta^d A_\nu^b A_\alpha^e}^{(0)}(q_4, q_2, q_1 + q_3) \\ &\quad - f^{ade} \Pi_{A_\nu^b A_\alpha^c A_\beta^e}^{(0)}(q_2, q_3, q_1 + q_4) \end{aligned} \quad (4.22)$$

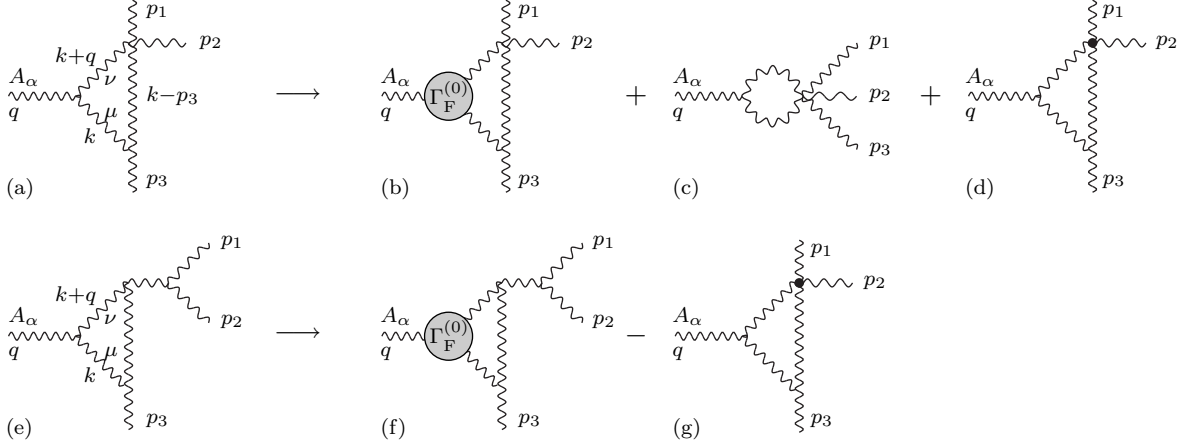


FIG. 6: The result of carrying out the PT decomposition on the 1PI four-point function $\Pi_{A_\alpha A_\beta A_\gamma A_\delta}^{A^2(1)}(p_1, p_2, p_3)$ (a) and the 1PR four-point function (b) for the case of three external on-shell gluons (permutations are not shown). Again, despite appearances, the vertex connecting the loop to the external gluons in diagrams (d) and (g), is a tree-gluon and not a four-gluon vertex.

When the PT decomposition is implemented in the graph of Fig.6e, it gives rise to various contributions, the most characteristic of which are depicted in Fig.6. Most notably, the parts of the WI which in the three-gluon vertex of the previous process that we considered were vanishing on-shell, because they were proportional to p_i^2 , now they simply cancel the off-shell propagator $d(p_1 + p_2)$, thus giving rise to the effectively 1PI graph shown in Fig.6g. This latter contribution will cancel exactly against the one shown in Fig.6d. It is important to notice at this point how all the above cancellations are encoded in the identities of Eqs.(3.32) and (3.36). In particular, the three last terms appearing on the RHS of Eq.(3.36) are nothing but the terms collectively depicted in Fig.6d, together with all the relevant permutations (not shown). Similarly, the two last terms on the RHS of Eq.(3.32) are precisely the terms shown in Fig.6d, which would have vanished if the external legs had been on-shell [as happens in Eq.(3.33)]. Notice that all these terms are proportional to the same basic quantity, namely the three-point function $\Pi_{\Omega A^* A}^{(1)}(q_1, q_2)$.

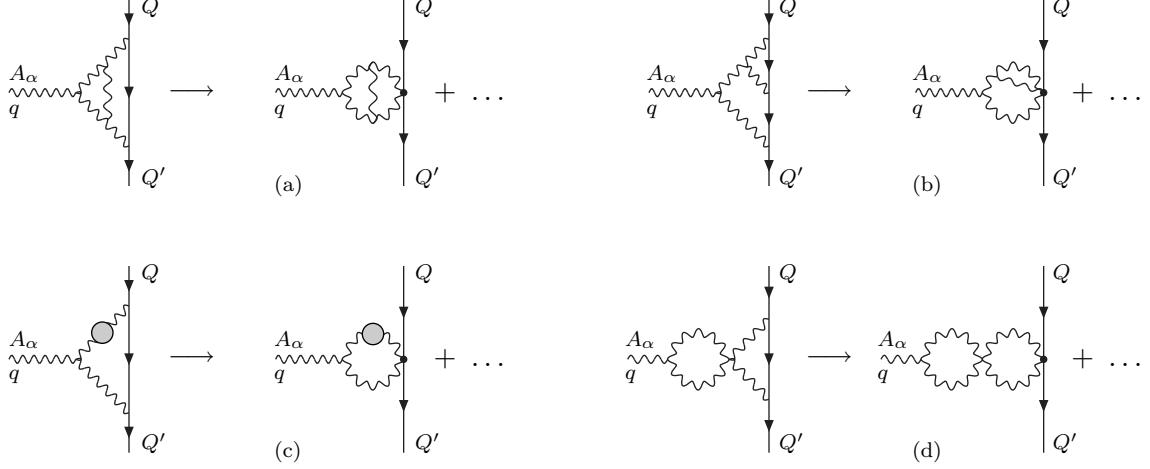


FIG. 7: Enforcing the PT decomposition on the three-point function $\Pi_{A\bar{\psi}\psi}^{A^2(2)}(Q', Q)$, gives rise to the topologies I_1 (a), I_3 (b), I_4 (c) and I_2 (d) of Eq.(5.2). The ellipses represents terms that whether they cancel or they modify the ghost structure.

V. TWO-LOOP CASE REVISITED

At the two-loop level [23, 24] we start again by carrying out the decomposition Eq.(4.10) of the two-loop three-point function $\Pi_{A\alpha\bar{\psi}\psi}^{(2)}(Q', Q)$; now all four categories of diagrams appearing on the RHS of Eq.(4.10) are non-vanishing. Next (see Fig.7), we implement the vertex decomposition Eq.(4.6) inside the $\Gamma_{A\alpha\bar{\psi}\psi}^{A^2(2)}(Q', Q)$ part, which will again trigger elementary WIs, leading us to the result

$$\Gamma_{A\alpha\bar{\psi}\psi}^{A^2(2)}(Q', Q) = \hat{\Gamma}_{A\alpha\bar{\psi}\psi}^{A^2(2)}(Q', Q) + \frac{1}{2}V_{\alpha\rho}^{P(2)}(q)\gamma^\rho + \frac{1}{2}F_\alpha^{P(2)}(Q, Q'), \quad (5.1)$$

with

$$\begin{aligned} V_{\alpha\rho}^{P(2)}(q) &= I_4 L_{\alpha\rho}(\ell, k) + (2I_2 + I_3)g_{\alpha\rho} \\ &\quad - I_1 [k_\rho g_{\alpha\sigma} + \Gamma_{\sigma\rho\alpha}^{(0)}(-k, -\ell, k + \ell)] (\ell - q)^\sigma, \\ F_\alpha^{P(2)}(Q', Q) &= d(q)\Pi_\alpha^{P(1)\beta}(q)\hat{\Pi}_{A\beta\bar{\psi}\psi}^{(1)}(Q', Q) + Y_\alpha^{P(2)}(Q', Q), \\ Y_P^{(2)}(Q', Q) &= X_{1\alpha}^{(1)}(Q', Q)\Sigma^{(1)}(Q') + \Sigma^{(1)}(Q)X_{2\alpha}^{(1)}(Q', Q). \end{aligned} \quad (5.2)$$

The integrals I_i appearing in Eq.(5.2) are defined as

$$\begin{aligned} iI_1 &= g^4 C_A^2 \int_{L_2} [\ell^2 (\ell - q)^2 k^2 (k + \ell)^2 (k + \ell - q)^2]^{-1}, \\ iI_2 &= g^4 C_A^2 \int_{L_2} [\ell^2 (\ell - q)^2 k^2 (k + q)^2]^{-1}, \end{aligned}$$

$$\begin{aligned}
iI_3 &= g^4 C_A^2 \int_{L_2} [\ell^2 (\ell - q)^2 k^2 (k + \ell)^2]^{-1}, \\
iI_4 &= g^4 C_A^2 \int_{L_2} [\ell^2 \ell^2 (\ell - q)^2 k^2 (k + \ell)^2]^{-1},
\end{aligned} \tag{5.3}$$

where we have defined the (two-loop) integral measure

$$\int_{L_2} \equiv (\mu^{2\varepsilon})^2 \int \frac{d^d k}{(2\pi)^d} \int \frac{d^d \ell}{(2\pi)^d}. \tag{5.4}$$

As before the term $Y_\alpha^{P(2)}(Q', Q)$ will vanish for on-shell external fermions so that it will be omitted all together. The term $\frac{1}{2}V_{\alpha\rho}^{P(2)}(q)\gamma^\rho$ represents the total propagator-like term originating from the two-loop three-point function $\Pi_{A_\alpha\bar{\psi}\psi}^{(2)}(Q', Q)$: together with the equal contribution coming from the mirror set of two-loop vertex diagrams, will give rise to the self-energy term

$$\Pi_{\alpha\beta}^{P(2)}(q) = q^2 V_{\alpha\rho}^{P(2)}(q) P_\beta^\rho(q), \tag{5.5}$$

which will be part of the two-loop PT gluon two-point function.

However beyond one-loop, this is not the end of the story, since one has to take into account the conversion of 1PR strings of conventional two-point functions $\Pi_{AA}(q)$, into strings containing PT two-point functions $\hat{\Pi}_{AA}(q)$ [6, 7]. Actually the term $\frac{1}{2}F_\alpha^{P(2)}(Q', Q)$ appearing in Eq.(5.2) is half of the vertex-like necessary to cancel the corresponding term appearing during the aforementioned conversion (the other half will come from the mirror set of diagrams).

The PT two-loop two-point function is then given by

$$\hat{\Pi}_{A_\alpha A_\beta}^{(2)}(q) = \Pi_{A_\alpha A_\beta}^{(2)}(q) + \Pi_{\alpha\beta}^{P(2)}(q) - R_{\alpha\beta}^{P(2)}(q). \tag{5.6}$$

where $R_{\alpha\beta}^{P(2)}(q)$, which also stems from the conversion of the conventional 1PR string into a 1PR PT one, is given by

$$iR_{\alpha\beta}^{P(2)}(q) = \Pi_{A_\alpha A_\rho}^{(1)}(q) V_\beta^{P(1)\rho}(q) + \frac{3}{4} V_{\alpha\rho}^{P(1)}(q) V_\beta^{P(1)\rho}(q). \tag{5.7}$$

Correspondingly, the two-loop PT three-point function $\hat{\Pi}_{A_\alpha\bar{\psi}\psi}^{(2)}(Q', Q)$ will be defined as

$$\begin{aligned}
\hat{\Pi}_{A_\alpha\bar{\psi}\psi}^{(2)}(Q', Q) &= \hat{\Gamma}_{A_\alpha\bar{\psi}\psi}^{A^2(2)}(Q', Q) + \Gamma_{A_\alpha\bar{\psi}\psi}^{\bar{c}c(2)}(Q', Q) + \Gamma_{A_\alpha\bar{\psi}\psi}^{A^3(2)}(Q', Q) + \Gamma_{A_\alpha\bar{\psi}\psi}^{\bar{q}q(2)}(Q', Q) \\
&= \Pi_{A_\alpha\bar{\psi}\psi}^{(2)}(Q', Q) + \frac{1}{2}V_{\alpha\rho}^{P(2)}(q)\gamma^\rho + \frac{1}{2}d(q)\Pi_\alpha^{P(1)\rho}(q)\hat{\Pi}_{A_\rho\bar{\psi}\psi}^{(1)}(Q', Q).
\end{aligned} \tag{5.8}$$

We can now compare these results with the one coming from the BQIs, so that we will be able to verify directly that

$$\widehat{\Pi}_{A_\alpha A_\beta}^{(2)}(q) \equiv \Pi_{\widehat{A}_\alpha \widehat{A}_\beta}^{(2)}(q), \quad (5.9)$$

$$\widehat{\Pi}_{A_\alpha \bar{\psi}\psi}^{(2)}(Q', Q) \equiv \Pi_{\widehat{A}_\alpha \bar{\psi}\psi}^{(2)}(Q', Q). \quad (5.10)$$

At the two-loop level the BQIs of Eqs.(3.22) and (3.30) read

$$\begin{aligned} \Pi_{\widehat{A}_\alpha \widehat{A}_\beta}^{(2)}(q) &= \Pi_{A_\alpha A_\beta}^{(2)}(q) + 2\Pi_{\Omega_\beta A_\rho^*}^{(2)}(q)\Pi_{A^\rho A_\alpha}^{(0)}(q) + 2\Pi_{\Omega_\beta A_\rho^*}^{(1)}(q)\Pi_{A^\rho A_\alpha}^{(1)}(q) \\ &\quad + \Pi_{\Omega_\alpha A_\rho^*}^{(1)}(q)\Pi_{A^\rho A^\sigma}^{(0)}(q)\Pi_{\Omega_\beta A_\sigma^*}^{(1)}(q), \end{aligned} \quad (5.11)$$

$$\begin{aligned} \Pi_{\widehat{A}_\alpha \bar{\psi}\psi}^{(2)}(Q', Q) &= \Pi_{A_\alpha \bar{\psi}\psi}^{(2)}(Q', Q) + \Pi_{\Omega_\alpha A_\rho^*}^{(2)}(q)\Pi_{A^\rho \bar{\psi}\psi}^{(0)}(Q', Q) \\ &\quad + \Pi_{\Omega_\alpha A_\rho^*}^{(1)}(q)\Pi_{A^\rho \bar{\psi}\psi}^{(1)}(Q', Q). \end{aligned} \quad (5.12)$$

Consider then Eq.(5.11). We will now prove that

$$\Pi_{\alpha\beta}^{\text{P}(2)}(q) - R_{\alpha\beta}^{\text{P}(2)}(q) = 2\Pi_{\Omega_\beta A_\rho^*}^{(2)}(q)\Pi_{A^\rho A_\alpha}^{(0)}(q) + 2\Pi_{\Omega_\beta A_\rho^*}^{(1)}(q)\Pi_{A^\rho A_\alpha}^{(1)}(q) + \left[\Pi_{\Omega_\alpha A_\rho^*}^{(1)}(q)\right]^2 \Pi_{A_\alpha A_\beta}^{(0)}(q). \quad (5.13)$$

To this end we notice that the left-hand side above can be written as

$$\begin{aligned} \Pi_{\alpha\beta}^{\text{P}(2)}(q) - R_{\alpha\beta}^{\text{P}(2)}(q) &= q^2 P_\beta^\rho(q) \left\{ I_4 L_{\alpha\rho}(\ell, k) + I_3 g_{\alpha\rho} \right. \\ &\quad \left. - I_1 [k_\rho g_{\alpha\sigma} + \Gamma_{\sigma\rho\alpha}^{(0)}(-k, -\ell, k + \ell)] (\ell - q)^\sigma \right\} \\ &\quad + iV_\beta^{\text{P}(1)\rho}(q)\Pi_{A_\rho A_\alpha}^{(1)}(q) - q^2 I_2 P_{\alpha\beta}(q). \end{aligned} \quad (5.14)$$

Then Eq.(4.19) implies

$$\begin{aligned} 2\Pi_{\Omega_\beta A_\rho^*}^{(1)}(q)\Pi_{A^\rho A_\alpha}^{(1)}(q) &= iV_\beta^{\text{P}(1)\rho}(q)\Pi_{A_\rho A_\alpha}^{(1)}(q), \\ \Pi_{\Omega_\alpha A_\rho^*}^{(1)}(q)\Pi_{A^\rho A^\sigma}^{(0)}(q)\Pi_{\Omega_\beta A_\sigma^*}^{(1)}(q) &= -q^2 I_2 P_{\alpha\beta}(q). \end{aligned} \quad (5.15)$$

Finally, from the perturbative expansion (3.23) one has that

$$i\Pi_{\Omega_\alpha A_\rho^*}^{(2)}(q) = \text{(a)} + \text{(b)} + \text{(c)} + \text{(d)}$$

where the blobs represent one-loop correction to the corresponding propagator. Using the Feynman rules of Fig.1, it is then straightforward to establish the following identities

$$\begin{aligned} \text{(a)} &= \frac{1}{2} I_1 \Gamma_{\sigma\rho\alpha}^{(0)}(-k, -\ell, k + \ell) (\ell - q)^\sigma, & \text{(b)} &= \frac{1}{2} I_1 (\ell - q)_\alpha k_\rho, \\ \text{(c)} &= -\frac{1}{2} I_4 L_{\alpha\rho}(\ell, k), & \text{(d)} &= -\frac{1}{2} I_3 g_{\alpha\rho}, \end{aligned} \quad (5.16)$$

so that

$$2\Pi_{\Omega_\beta A_\rho^*}^{(2)}(q)\Pi_{A^\rho A_\alpha}^{(0)}(q) = q^2 P_\beta^\rho(q) \left\{ I_4 L_{\alpha\rho}(\ell, k) + I_3 g_{\alpha\rho} \right. \\ \left. - I_1 [k_\rho g_{\alpha\sigma} + \Gamma_{\sigma\rho\alpha}^{(0)}(-k, -\ell, k + \ell)] (\ell - q)^\sigma \right\}. \quad (5.17)$$

Thus Eq.(5.9) is proved.

Finally consider the two-loop PT three-point function Eq.(5.8), which using Eq.(4.17), reads

$$\hat{\Pi}_{A_\alpha \bar{\psi}\psi}^{(2)}(Q', Q) = \Pi_{A_\alpha \bar{\psi}\psi}^{(2)}(Q', Q) + \frac{i}{2} V_\alpha^{P(1)\rho}(q) \Pi_{A_\rho \bar{\psi}\psi}^{(1)} - \frac{1}{2} \left\{ I_4 L_{\alpha\rho}(\ell, k) + I_3 g_{\alpha\rho} \right. \\ \left. - I_1 [k_\rho g_{\alpha\sigma} + \Gamma_{\sigma\rho\alpha}^{(0)}(-k, -\ell, k + \ell)] (\ell - q)^\sigma \right\} \gamma^\rho. \quad (5.18)$$

Then using Eqs.(4.19) and (5.16) we get

$$\Pi_{\Omega_\alpha A_\rho^*}^{(1)}(q) \Pi_{A^\rho \bar{\psi}\psi}^{(1)}(Q', Q) = \frac{i}{2} V_\alpha^{P(1)\rho}(q) \Pi_{A_\rho \bar{\psi}\psi}^{(1)}, \\ \Pi_{\Omega_\alpha A_\rho^*}^{(2)}(q) \Pi_{A^\rho \bar{\psi}\psi}^{(0)}(Q', Q) = \frac{1}{2} \left\{ I_4 L_{\alpha\rho}(\ell, k) + I_3 g_{\alpha\rho} \right. \\ \left. - I_1 [k_\rho g_{\alpha\sigma} + \Gamma_{\sigma\rho\alpha}^{(0)}(-k, -\ell, k + \ell)] (\ell - q)^\sigma \right\} \gamma^\rho, \quad (5.19)$$

so that Eq.(5.10) is also proved.

VI. A NEW RESULT: THE TWO-LOOP INTRINSIC PINCH TECHNIQUE

In the intrinsic PT construction one avoids the embedding of the PT objects into S -matrix elements; of course, all results of the intrinsic PT are identical to those obtained in the S -matrix PT context. The basic idea, is that the pinch graphs, which are essential in canceling the gauge dependences of ordinary diagrams, are always missing one or more propagators corresponding to the external legs of the improper Green's function in question. It then follows that the gauge-dependent parts of such ordinary diagrams must also be missing one or more external propagators. Thus the intrinsic PT construction goal is to isolate systematically the parts of 1PI diagrams that are proportional to the inverse propagators of the external legs and simply discard them. The important point is that these inverse propagators arise from the STI satisfied by the three-gluon vertex appearing inside appropriate sets of diagrams, when it is contracted by longitudinal momenta. The STI triggered

is nothing but Eq.(3.10), *i.e.*,

$$\begin{aligned}
p_1^\mu \mathbb{I}_{A_\alpha A_\mu A_\nu}(q, p_1, p_2) &= [i\Delta_\nu^{(-1)\rho}(p_2) + p_2^\rho p_{2\nu}] [p_1^2 D(p_1)] H_{\rho\alpha}(p_2, q) \\
&\quad - [i\Delta_\alpha^{(-1)\rho}(q) + q^\rho q_\alpha] [p_1^2 D(p_1)] H_{\rho\nu}(q, p_2), \\
p_2^\nu \mathbb{I}_{A_\alpha A_\mu A_\nu}(q, p_1, p_2) &= [i\Delta_\alpha^{(-1)\rho}(q) + q^\rho q_\alpha] [p_2^2 D(p_2)] H_{\rho\mu}(q, p_1) \\
&\quad - [i\Delta_\mu^{(-1)\rho}(p_1) + p_1^\rho p_{1\mu}] [p_2^2 D(p_2)] H_{\rho\alpha}(p_1, q), \tag{6.1}
\end{aligned}$$

where the momenta p_1^μ and p_2^ν are now related to virtual integration momenta appearing in the quantum loop. This construction has been carried out at one-loop in [2] where only the tree-level version of Eq.(3.10), namely Eq.(3.11), has been invoked. Here we present for the first time the two-loop generalization of this construction, employing the one-loop version of Eq.(3.10). In addition to proving that the one-loop construction can in fact be generalized to two-loops, a non-trivial result in its own right, we present a different but equivalent point of view to that of [1], motivated by the BV formalism in general, and the BQIs presented in Section II in particular. The novel ingredient we present here is the following: The essential feature of the intrinsic PT construction is to arrive at the desired object, for example the effective gluon self-energy by discarding pieces from the conventional self-energy. The terms discarded originate from the RHS of Eq.(3.10), and, according to the discussion presented in Section II, they are all precisely known in terms of physical and unphysical Green's functions, appearing in the theory. Then, by virtue of identifications such as those given in Eqs.(3.14), (3.15), and (3.18), one can directly compare the result obtained by the intrinsic PT procedure to the corresponding BFM quantity (at $\xi_Q = 1$), employing the BQI of Eq.(3.22). We emphasize that at no point do we use the BQIs or the BV formalism in general in arriving at the intrinsic PT result; the BQIs are only a-posteriori invoked, at the end of the PT procedure, because they greatly facilitate the comparison with the BFM result. Last but not least, the two-loop construction presented here, provides additional evidence supporting the point of view adopted in [23, 24], namely that no internal vertex must be rearranged, and no pieces must be therefore discarded as a result of this rearrangement. The reason is simply that one needs to maintain the *full* one-loop three-gluon vertex, on which the momenta will act in order for Eq.(6.1) to be triggered; instead, if one were to remove pieces by modifying internal vertices [46], one would invariably distort the aforementioned STI.

We start by reviewing the one-loop intrinsic PT construction, beginning again, without

loss of generality, in the renormalizable Feynman gauge. Consider the one-loop gluon two-point function

$$\mathbb{I}_{A_\alpha A_\beta}^{(1)}(q) = \frac{1}{2} \int_{L_1} J(q, k) L_{\alpha\beta}(q, k), \quad (6.2)$$

where, after symmetrizing the ghost loop,

$$L_{\alpha\beta}(q, k) = \Gamma_{\alpha\mu\nu}^{(0)}(q, k, -k - q) \Gamma_\beta^{(0)\mu\nu}(q, k, -k - q) - k_\alpha (k + q)_\beta - k_\beta (k + q)_\alpha. \quad (6.3)$$

In the absence of longitudinal momenta coming from internal gluon propagators (since we work in the Feynman gauge), the only momenta that can trigger an STI come from the three-gluon vertices. We then carry out the PT decomposition of Eq.(4.6) on *both* the three-gluon vertices appearing at the two ends of the diagram, *i.e.*, we write

$$\begin{aligned} \Gamma_{\alpha\mu\nu}^{(0)} \Gamma_\beta^{(0)\mu\nu} &= [\Gamma_{\alpha\mu\nu}^F + \Gamma_{\alpha\mu\nu}^P][\Gamma_\beta^{F\mu\nu} + \Gamma_\beta^{P\mu\nu}] \\ &= \Gamma_{\alpha\mu\nu}^F \Gamma_\beta^{F\mu\nu} + \Gamma_{\alpha\mu\nu}^P \Gamma_\beta^{(0)\mu\nu} + \Gamma_{\alpha\mu\nu}^{(0)} \Gamma_\beta^{P\mu\nu} - \Gamma_{\alpha\mu\nu}^P \Gamma_\beta^{P\mu\nu}. \end{aligned} \quad (6.4)$$

Of the four terms of the equation above, the first and last are left untouched; for the second and third terms, using the three-gluon vertex STI of Eq.(6.1), we find

$$\begin{aligned} \Gamma_{\alpha\mu\nu}^P \Gamma_\beta^{(0)\mu\nu} + \Gamma_{\alpha\mu\nu}^{(0)} \Gamma_\beta^{P\mu\nu} &= -4iq^2 P_{\alpha\rho}(q) H_{\rho\beta}^{(0)}(q, -k - q) + 2ik^2 P_{\alpha\rho}(k) H_{\rho\beta}^{(0)}(k, q) \\ &\quad + 2i(k + q)^2 P_{\alpha\rho}(k + q) H_{\rho\beta}^{(0)}(-k - q, q) \\ &= -4q^2 P_{\alpha\beta}(q) + 2k^2 P_{\alpha\beta}(k) + 2(k + q)^2 P_{\alpha\beta}(k + q). \end{aligned} \quad (6.5)$$

where (after factoring out the coupling constant g) we have used that $H_{\alpha\beta}^{(0)} = -ig_{\alpha\beta}$. The first term on the RHS, to be denoted by $\Pi_{\alpha\beta}^{\text{IP}(1)}(q)$, where the superscript “IP” stands for “intrinsic pinch”, is to be discarded from the gluon self-energy. Thus, the 1PI one-loop intrinsic PT gluon self-energy, to be denoted as before by $\widehat{\mathbb{I}}_{A_\alpha A_\beta}^{(1)}(q)$, is defined as

$$\widehat{\mathbb{I}}_{A_\alpha A_\beta}^{(1)}(q) = \mathbb{I}_{A_\alpha A_\beta}^{(1)}(q) - \Pi_{\alpha\beta}^{\text{IP}(1)}(q) \quad (6.6)$$

Notice that $\Pi_{\alpha\beta}^{\text{IP}(1)}(q)$ has precisely the form

$$\Pi_{\alpha\beta}^{\text{IP}(1)}(q) = \frac{1}{2} [-4q^2 P_{\alpha\beta}(q)] \int_{L_1} J(q, k) = -\Pi_{\alpha\beta}^P(q), \quad (6.7)$$

so that dropping this term in Eq.(6.5) has the same effect of canceling it with the S -matrix PT. At this point in the original construction of [2] the first and last terms on the RHS of

Eq.(6.4) were combined with the second and third term on the RHS of Eq.(6.5), in order to show that, after elementary algebraic manipulations, $\widehat{\Pi}_{A_\alpha A_\beta}^{(1)}(q)$ assumes the form

$$\widehat{\Pi}_{A_\alpha A_\beta}^{(1)}(q) = \frac{1}{2} \int_{L_1} J_1(q, k) \widehat{L}_{\alpha\beta}(q, k), \quad (6.8)$$

with

$$\widehat{L}_{\alpha\beta}(q, k) \equiv \Gamma_{F\alpha}^{(0)\sigma\rho}(q, k, -k - q) \Gamma_{F\beta\sigma\rho}^{(0)}(q, k, -k - q) - 2(2k + q)_\alpha (2k + q)_\beta. \quad (6.9)$$

As was realized a few years later [20], this last expression of $\widehat{\Pi}_{A_\alpha A_\beta}^{(1)}(q)$ coincides with $\Pi_{\widehat{A}_\alpha \widehat{A}_\beta}^{(1)}(q)$. Notice however that, in view of the BQI of Eq.(3.22), this last identification is more immediate, in the sense that no further manipulation of the answer is needed: the difference between $\widehat{\Pi}_{A_\alpha A_\beta}^{(1)}(q)$ and $\Pi_{A_\alpha A_\beta}^{(1)}(q)$ is the same as the difference between $\Pi_{\widehat{A}_\alpha \widehat{A}_\beta}^{(1)}(q)$ and $\Pi_{A_\alpha A_\beta}^{(1)}(q)$, as given by the BQI. Thus, once $\widehat{\Pi}_{A_\alpha A_\beta}^{(1)}(q)$ has been constructed the BQI serves as a short-cut for relating it to $\Pi_{\widehat{A}_\alpha \widehat{A}_\beta}^{(1)}(q)$. Even though at one-loop the amount of algebra thusly saved is insignificant, at two-loops and beyond the use of the BQI constitutes a definite technical advantage.

Let us conclude the one-loop analysis by introducing a short-hand notation for the intrinsic PT construction, that will be useful in its two-loop generalization that will follow. We begin by writing the diagram of Fig.4a, suppressing all Lorentz and color indices, as

$$(\Gamma\Gamma) = (\Gamma^F\Gamma^F) + (\Gamma^P\Gamma) + (\Gamma\Gamma^P) - (\Gamma^P\Gamma^P). \quad (6.10)$$

Then using the tree-level STI of Eq.(6.1), we write

$$\begin{aligned} (\Gamma^P\Gamma) &= -iVd^{-1} + 2L, \\ (\Gamma\Gamma^P) &= -id^{-1}V + 2L, \end{aligned} \quad (6.11)$$

so that

$$(\Gamma\Gamma) = -2id^{-1}V + (\Gamma^F\Gamma^F) + 4L - (\Gamma^P\Gamma^P). \quad (6.12)$$

The quantities A and L , can be read off directly from Eq.(6.5), and are equal to

$$\begin{aligned} V_{\alpha\beta}(q) &= -2P_{\alpha\beta}(q) \int_{L_1} J(q, k), \\ L_{\alpha\beta}(q) &= \frac{1}{2} \int_{L_1} J(q, k) [k^2 P_{\alpha\beta}(k) + (k + q)^2 P_{\alpha\beta}(k + q)]. \end{aligned} \quad (6.13)$$

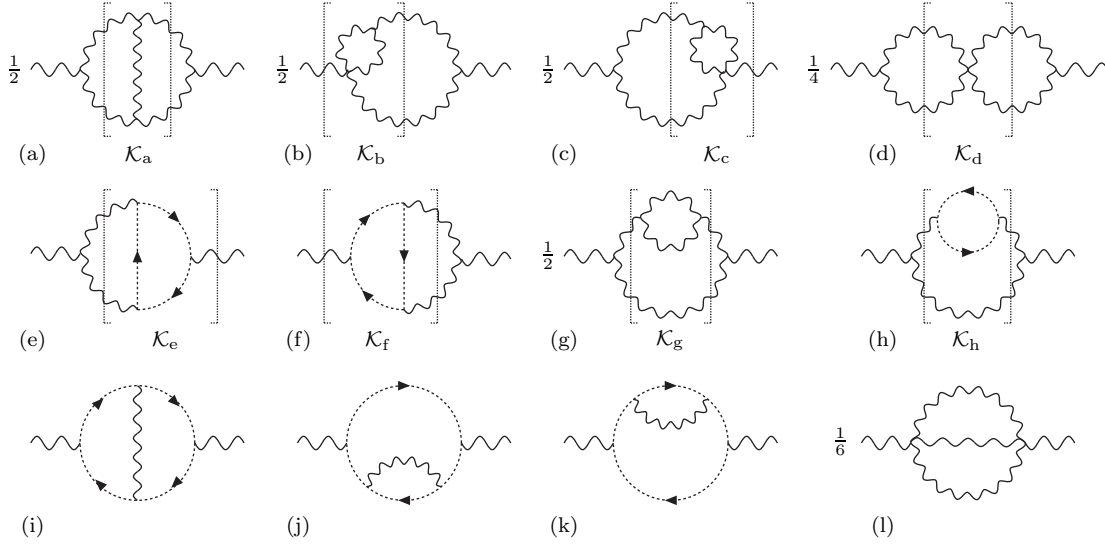


FIG. 8: The Feynman diagrams, together with their statistical weights and the associated kernels, contributing to the conventional two-loop gluon two-point function $\Pi_{A_\alpha A_\beta}^{(2)}(q)$ in the R_ξ gauges.

Moreover one has the well known one-loop PT result

$$(GG) + 2L - \frac{1}{2}(\Gamma^P \Gamma^P) = (\widehat{G}\widehat{G}), \quad (6.14)$$

where (GG) represents the ghost diagram of Fig.4b, and $(\widehat{G}\widehat{G})$ is the corresponding diagram with background ghost circulating in the loop. This will finally furnish the result

$$\begin{aligned} \Pi_{AA}^{(1)} &= \frac{1}{2}(\Gamma\Gamma) + (GG) \\ &= -id^{-1}V + \frac{1}{2}(\Gamma^F \Gamma^F) + (\widehat{G}\widehat{G}) \\ &= -\Pi^P{}^{(1)} + \Pi_{\widehat{A}\widehat{A}}^{(1)}. \end{aligned} \quad (6.15)$$

We will now generalize the intrinsic PT construction presented above, to two-loops. The 1PI Feynman diagrams contributing to the conventional two-loop gluon self-energy in the R_ξ gauges are represented in Fig.8. They can be separated into three distinct sets: (i) the set of diagrams that have two external (tree-level) three-gluon vertices, and thus can be written schematically (suppressing Lorentz indices) as $\Gamma^{(0)}[\mathcal{K}]\Gamma^{(0)}$, where \mathcal{K} is some kernel; to this set belong diagrams (a), (d), (g) and (h). (ii) the set of diagrams with only one external (tree-level) three-gluon vertex, and thus can be written as $\Gamma^{(0)}[\mathcal{K}]$ or $[\mathcal{K}]\Gamma^{(0)}$; this set is composed by the diagrams (b), (c), (e) and (f). (iii) All remaining diagrams, containing no external three-gluon vertices.

At this point we make the following observation: if one were to carry out the decomposition Eq.(6.4) to the pair of external vertices appearing in the diagrams of the set (i), and the decomposition of Eq.(4.6) to the external vertex appearing in the diagrams of the set (ii), after a judicious rearrangement of terms, the longitudinal terms p_1^μ and p_2^ν stemming from $\Gamma_{\alpha\mu\nu}^P(q, p_1, p_2)$ and/or $\Gamma_\beta^{P\mu\nu}(q, p_1, p_2)$ would be triggering the one-loop version of Eq.(6.1), just as in the one-loop case one has been triggering the tree-level version of Eq.(6.1). The only exception are of course diagrams (g) and (h), where the STI triggered is still the tree-level version of Eq.(6.1). Therefore, the straightforward generalization of the intrinsic PT to two-loops would amount to isolating from the two-loop diagrams the terms of the STI of Eq.(6.1) that are proportional to $[\Delta_\alpha^{(-1)\rho}(q)]^{(n)}$, with $n = 0, 1$; we will denote such contributions by $\Pi_{\alpha\beta}^{\text{IP}(2)}(q)$. Thus the 1PI diagrams contributing to the two-loop gluon self-energy can be cast in the form

$$\mathbb{I}_{A_\alpha A_\beta}^{(2)}(q) = G_{A_\alpha A_\beta}^{(2)}(q) + \Pi_{\alpha\beta}^{\text{IP}(2)}(q). \quad (6.16)$$

Notice however that the 1PR set of one-loop self-energy diagrams, *i.e.*, the strings shown in Fig.9, must also be rearranged following the intrinsic PT procedure, and be converted into the equivalent string involving PT one-loop self-energies (which are known objects from the one-loop results). As we will see in detail in what follows, this treatment of the 1PR strings will give rise, in addition to the PT strings, to (a) a set of contributions which are proportional to the inverse propagator of the external legs $d^{-1}(q)$, and (b) a set of contributions which is *effectively* 1PI, and therefore also belongs to the definition of the 1PI two-loop PT gluon self-energy; we will denote these two sets of contributions collectively by $S_{\alpha\beta}^{\text{IP}(2)}(q)$. Thus the sum of the 1PI and 1PR contributions to the conventional two-loop gluon self-energy can be cast in the form

$$\begin{aligned} \mathbb{I}_{A_\alpha A_\beta}^{(2)}(q) + \mathbb{I}_{A_\alpha A_\rho}^{(1)}(q)d(q)\mathbb{I}_{A^\rho A_\beta}^{(1)}(q) &= G_{A_\alpha A_\beta}^{(2)}(q) + \widehat{\mathbb{I}}_{A_\alpha A_\rho}^{(1)}(q)d(q)\widehat{\mathbb{I}}_{A^\rho A_\beta}^{(1)}(q) \\ &+ \Pi_{\alpha\beta}^{\text{IP}(2)}(q) + S_{\alpha\beta}^{\text{IP}(2)}(q). \end{aligned} \quad (6.17)$$

By definition of the intrinsic PT procedure, we will now discard from the above expression all the terms which are proportional to the inverse propagator of the external legs $d^{-1}(q)$, thus defining the quantity

$$R_{\alpha\beta}^{\text{IP}(2)}(q) = \Pi_{\alpha\beta}'^{\text{IP}(2)}(q) + S_{\alpha\beta}'^{\text{IP}(2)}(q), \quad (6.18)$$

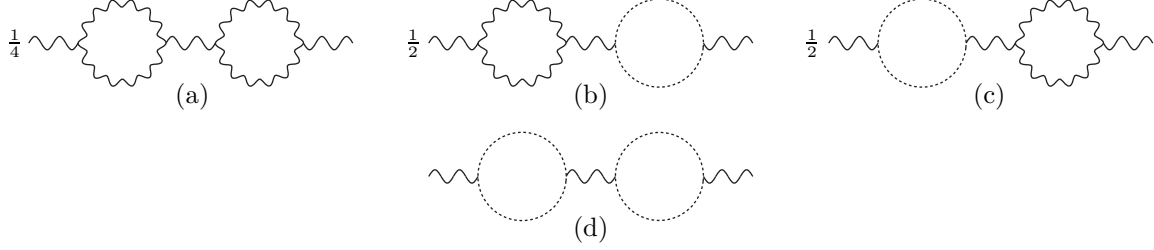


FIG. 9: The two-loop 1PR strings (together with their statistical weights) in the R_ξ gauges.

where the primed functions are defined starting from the unprimed ones appearing in Eq.(6.17) by discarding the aforementioned terms.

Thus, making use of Eqs.(6.16), (6.17) and (6.18), the 1PI two-loop intrinsic PT gluon self-energy, to be denoted as before by $\widehat{\Pi}_{A_\alpha A_\beta}^{(2)}(q)$, is defined as

$$\begin{aligned}\widehat{\Pi}_{A_\alpha A_\beta}^{(2)}(q) &= G_{A_\alpha A_\beta}^{(2)}(q) + R_{\alpha\beta}^{\text{IP}(2)}(q) \\ &= \Pi_{A_\alpha A_\beta}^{(2)}(q) - \Pi_{\alpha\beta}^{\text{IP}(2)}(q) + R_{\alpha\beta}^{\text{IP}(2)}(q).\end{aligned}\quad (6.19)$$

Of course the quantities $\widehat{\Pi}_{A_\alpha A_\beta}^{(2)}(q)$ and $\Pi_{A_\alpha A_\beta}^{(2)}(q)$ appearing on the RHS of Eqs.(5.6) and (6.19) are identical; however, the result of Eq.(6.7) does not generalize beyond one-loop. Thus, at two-loops $-\Pi_{\alpha\beta}^{\text{IP}(2)}(q) \neq \Pi_{\alpha\beta}^{\text{P}(2)}(q)$ and $R_{\alpha\beta}^{\text{IP}(2)}(q) \neq R_{\alpha\beta}^{\text{P}(2)}(q)$; however

$$-\Pi_{\alpha\beta}^{\text{IP}(2)}(q) + R_{\alpha\beta}^{\text{IP}(2)}(q) \equiv \Pi_{\alpha\beta}^{\text{P}(2)}(q) - R_{\alpha\beta}^{\text{P}(2)}(q). \quad (6.20)$$

We next proceed to give the details of the construction of the quantities $\Pi_{\alpha\beta}^{\text{IP}(2)}(q)$ and $R_{\alpha\beta}^{\text{IP}(2)}(q)$ discussed above, starting from the first one.

As a first step, we carry out the usual PT decomposition of the three-gluon vertex to the graphs of set (i) and (ii). Taking into account the statistical factors, for diagrams (a) and (d) we then obtain

$$\begin{aligned}\frac{1}{2}\Gamma^{(0)}[\mathcal{K}_a + \tfrac{1}{2}\mathcal{K}_d]\Gamma^{(0)} &= \frac{1}{2}\Gamma^{\text{F}}[\mathcal{K}_a + \tfrac{1}{2}\mathcal{K}_d]\Gamma^{\text{F}} + \frac{1}{2}\Gamma^{\text{P}}[\mathcal{K}_a + \tfrac{1}{2}\mathcal{K}_d]\Gamma^{(0)} \\ &+ \frac{1}{2}\Gamma^{(0)}[\mathcal{K}_a + \tfrac{1}{2}\mathcal{K}_d]\Gamma^{\text{P}} - \frac{1}{2}\Gamma^{\text{P}}[\mathcal{K}_a + \tfrac{1}{2}\mathcal{K}_d]\Gamma^{\text{P}}.\end{aligned}\quad (6.21)$$

As in the one-loop case, of the four terms appearing above the first and last term remain untouched, and constitute part of the answer. To the second and third terms we add the Γ^{P} part of diagrams (c), (e) and (b), (f) respectively to get

$$\begin{aligned}[(\text{ii}) + (\text{c}) + (\text{e})]^{\text{P}} &= \frac{1}{2}\Gamma^{\text{P}}[\mathcal{K}_a\Gamma^{(0)} + \tfrac{1}{2}\mathcal{K}_d\Gamma^{(0)} + \mathcal{K}_c + 2\mathcal{K}_e], \\ [(\text{iii}) + (\text{b}) + (\text{f})]^{\text{P}} &= [\Gamma^{(0)}\mathcal{K}_a + \Gamma^{(0)}\tfrac{1}{2}\mathcal{K}_d + \mathcal{K}_b + 2\mathcal{K}_f]\tfrac{1}{2}\Gamma^{\text{P}}.\end{aligned}\quad (6.22)$$

It is then straightforward to see that the two contribution are actually equal, and moreover that

$$\begin{aligned} & \mathcal{K}_a \Gamma^{(0)} + \frac{1}{2} \mathcal{K}_d \Gamma^{(0)} + \mathcal{K}_c + 2\mathcal{K}_e = \\ & \begin{array}{c} \text{Diagram 1} + \frac{1}{2} \text{Diagram 2} + \frac{1}{2} \text{Diagram 3} + \frac{1}{2} \text{Diagram 4} + \text{Diagram 5} + \text{Diagram 6} \\ \equiv \mathbb{I}_{AAA}^{(1)}. \end{array} \end{aligned}$$

Thus, inserting back the Lorentz structure, we get the equation

$$[(\text{ii}) + (\text{c}) + (\text{e}) + (\text{iii}) + (\text{b}) + (\text{f})]^P = \int_{L_1} J(k, q) \Gamma_{\alpha\mu\nu}^P(q, k, -k - q) \mathbb{I}_{A\beta A^\mu A^\nu}^{(1)}(q, k, -k - q). \quad (6.23)$$

For the remaining two first class diagrams (g) and (h), we carry out the same decomposition as for diagrams (a) and (d), concentrating again only on the terms

$$[(\text{g}) + (\text{h})]^P = \Gamma^P [\frac{1}{2} \mathcal{K}_g + \mathcal{K}_h] \Gamma^{(0)} + \Gamma^{(0)} [\frac{1}{2} \mathcal{K}_g + \mathcal{K}_h] \Gamma^P. \quad (6.24)$$

Next, one notices that the two contributions are actually equal, and moreover that

$$[\frac{1}{2} \mathcal{K}_g + \mathcal{K}_h] \Gamma^{(0)} = \begin{array}{c} \text{Diagram with blob} \end{array} \quad (6.25)$$

where the blob represent the one-loop correction to the gluon propagator. Inserting back the Lorentz structure, we then get the equation

$$[(\text{g}) + (\text{h})]^P = 2 \int_{L_1} J(k, q) \Gamma_{\alpha\mu\nu}^P(q, k, -k - q) \mathbb{I}_{A^\mu A_\rho}^{(1)}(k) d(k) \Gamma_\beta^{(0)\rho\nu}(q, k, -k - q). \quad (6.26)$$

Eqs.(6.23) and (6.26) will then be our starting point: from them, by using the three-gluon vertex STI of Eq.(6.1), we will isolate the 1PI parts that are proportional to the inverse propagator of the external leg, and simply discard them.

Let us start from Eq.(6.23). From Eq.(4.7) and the one-loop version of Eq.(6.1) we find

$$\begin{aligned} \Gamma_{\alpha\mu\nu}^P(q, k, -k - q) \mathbb{I}_{A\beta A^\mu A^\nu}^{(1)}(q, k, -k - q) &= 2H_{\rho\alpha}^{(0)}(q, -k - q) \mathbb{I}_{A^\rho A_\beta}^{(1)}(q) \\ &\quad - 2q^2 H_{\rho\alpha}^{(0)}(q, -k - q) P_\beta^\rho(q) [k^2 D^{(1)}(k)] \\ &\quad - 2iq^2 H_{\rho\alpha}^{(1)}(q, -k - q) P_\beta^\rho(q) + \dots, \end{aligned} \quad (6.27)$$

where the ellipses stands for terms that will be part of the two-loop function $G_{A_\alpha A_\beta}^{(2)}(q)$. The perturbative expansion of the function H , will give

$$H_{\rho\beta}^{(1)}(q, -k - q) = \text{Diagram 1} + \text{Diagram 2}$$

so that, using the Feynman rules given in Fig.1, we find

$$\int_{L_1} J(q, k) \left[2H_{\rho\alpha}^{(0)}(q, -k - q) \mathbb{I}_{A_\rho A_\beta}^{(1)}(q) \right] = -i \mathbb{I}_{A_\alpha A_\rho}^{(1)}(q) V_\beta^{P(1)\rho}(q), \quad (6.28)$$

$$\int_{L_1} J(q, k) \left\{ -2q^2 H_{\rho\alpha}^{(0)}(q, -k - q) P_\beta^\rho(q) [k^2 D^{(1)}(k)] \right\} = -q^2 P_{\alpha\beta}(q) I_3, \quad (6.29)$$

$$\int_{L_1} J(q, k) \left[-2iq^2 H_{\rho\alpha}^{(1)}(q, -k - q) P_\beta^\rho(q) \right] = q^2 I_1 \{ [k_\rho g_{\alpha\sigma} + \Gamma_{\sigma\rho\alpha}^{(0)}(-k, -\ell, k + \ell)] (\ell - q)^\sigma \} P_\beta^\rho(q). \quad (6.30)$$

Next consider the lower order corrections of Eq.(6.26). From Eq.(4.7) and the fact that the gluon two-point function is transverse at all orders, we find

$$\begin{aligned} \Gamma_{\alpha\mu\nu}^P(q, k, -k - q) \mathbb{I}_{A^\mu A_\rho}^{(1)}(k) \Gamma_\beta^{(0)\rho\nu}(q, k, -k - q) \\ = -(k + q)_\nu \mathbb{I}_{A_\alpha A_\rho}^{(1)}(k) \Gamma_\beta^{(0)\rho\nu}(q, k, -k - q), \end{aligned} \quad (6.31)$$

so that using the tree-level version of the STI of Eq.(6.1) and isolating the term which will be discarded, we have

$$2J(q, k) \mathbb{I}_{A_\alpha A_\rho}^{(1)}(k) d(k) \left[-iq^2 P_\beta^\sigma(q) H_{\sigma\rho}^{(0)}(q, k) \right] = -q^2 P_\beta^\rho(q) I_4 L_{\alpha\rho}(\ell, k). \quad (6.32)$$

Collecting the terms on the RHS of Eqs.(6.28)–(6.32) we finally obtain

$$\begin{aligned} \Pi_{\alpha\beta}^{\text{IP}(2)}(q) &= -i \mathbb{I}_{A_\alpha A_\rho}^{(1)}(q) V_\beta^{P(1)\rho}(q) - q^2 P_{\alpha\beta}(q) I_3 - q^2 P_\beta^\rho(q) I_4 L_{\alpha\rho}(\ell, k) \\ &+ q^2 P_\alpha^\rho(q) I_1 [k_\rho g_{\alpha\sigma} + \Gamma_{\sigma\rho\beta}^{(0)}(-k, -\ell, k + \ell)] (\ell - q)^\sigma \end{aligned} \quad (6.33)$$

Next we turn to the contributions coming from the the conversion of the conventional two-loop 1PR strings to PT 1PR strings, and determine the quantity $S_{\alpha\beta}^{\text{IP}(2)}(q)$. Using the notation introduced in the one-loop case we find for the diagram of Fig.9a the result

$$\begin{aligned} (5a) &= (\Gamma\Gamma) d_i (\Gamma\Gamma) \\ &= (\Gamma^F \Gamma^F) d_i (\Gamma^F \Gamma^F) - (\Gamma^F \Gamma^F) d_i (\Gamma^P \Gamma^P) - (\Gamma^P \Gamma^P) d_i (\Gamma^F \Gamma^F) + (\Gamma^P \Gamma^P) d_i (\Gamma^P \Gamma^P) \end{aligned}$$

$$\begin{aligned}
& + 4(\Gamma^F \Gamma^F) d_i L + 4L d_i (\Gamma^F \Gamma^F) - 4(\Gamma^P \Gamma^P) d_i L - 4L d_i (\Gamma^P \Gamma^P) + 16L d_i L \\
& - i(\Gamma^F \Gamma^F) d_i V d^{-1} - i d^{-1} V d_i (\Gamma^F \Gamma^F) + i d^{-1} V d_i (\Gamma^P \Gamma^P) + i(\Gamma^P \Gamma^P) d_i V d^{-1} \\
& - d^{-1} V d_i V d^{-1} - 4i d^{-1} V d_i L - 4i L d_i V d^{-1} \\
& + V d_i^{-1} V - iV(\Gamma\Gamma) - i(\Gamma\Gamma)V.
\end{aligned} \tag{6.34}$$

Here we have made an explicit distinction between the *internal* propagator d_i and the external ones d : The presence or absence of the former will determine if the corresponding diagram has to be considered 1PR or 1PI respectively. For the remaining diagrams we then get

$$\begin{aligned}
(5b) &= (\Gamma\Gamma) d_i (GG) \\
&= (\Gamma^F \Gamma^F) d_i (GG) - (\Gamma^P \Gamma^P) d_i (GG) + 4L d_i (GG) - i d^{-1} V d_i (GG) - iV(GG), \\
(5c) &= (GG) d_i (\Gamma\Gamma) \\
&= (GG) d_i (\Gamma^F \Gamma^F) - (GG) d_i (\Gamma^P \Gamma^P) + 4(GG) d_i L - i(GG) d_i V d^{-1} - i(GG)V.
\end{aligned} \tag{6.35}$$

We can then start collecting pieces. Recalling the statistical weight of each diagram of Fig.9, and using the one-loop result of Eq.(6.14), we find

$$\begin{aligned}
\frac{1}{2}(\Gamma^F \Gamma^F) d_i (\widehat{G}\widehat{G}) &= \frac{1}{2}(\Gamma^F \Gamma^F) d_i \left[(GG) + 2L - \frac{1}{2}(\Gamma^P \Gamma^P) \right], \\
\frac{1}{2}(\widehat{G}\widehat{G}) d_i (\Gamma^F \Gamma^F) &= \frac{1}{2} \left[(GG) + 2L - \frac{1}{2}(\Gamma^P \Gamma^P) \right] d_i (\Gamma^F \Gamma^F), \\
(\widehat{G}\widehat{G}) d_i (\widehat{G}\widehat{G}) &= (GG) d_i (GG) + (GG) d_i \left[2L - \frac{1}{2}(\Gamma^P \Gamma^P) \right] + \left[2L - \frac{1}{2}(\Gamma^P \Gamma^P) \right] d_i (GG) \\
&\quad + 4L d_i L - L d_i (\Gamma^P \Gamma^P) - (\Gamma^P \Gamma^P) d_i L + \frac{1}{4}(\Gamma^P \Gamma^P) d_i (\Gamma^P \Gamma^P).
\end{aligned} \tag{6.36}$$

These terms together with the first term of Eq.(6.34), will give the PT 1PR string. For the genuine 1PI terms we have instead the following result

$$\frac{1}{4}V d_i^{-1} V - \frac{1}{4}iV(\Gamma\Gamma) - \frac{1}{4}i(\Gamma\Gamma)V - \frac{1}{2}iV(GG) - \frac{1}{2}i(GG)V = \frac{1}{4}V d_i^{-1} V - iV\mathbb{T}_{AA}^{(1)}, \tag{6.37}$$

so that by adding to them the remaining terms proportional to the *external* inverse propagator $d^{-1}(q)$, we will get the quantity

$$\begin{aligned}
S^{\text{IP}(2)}(q) &= \frac{1}{4}V d_i^{-1} V - iV\mathbb{T}_{AA}^{(1)} \\
&\quad - i(\Gamma^F \Gamma^F) d_i V d^{-1} - i d^{-1} V d_i (\Gamma^F \Gamma^F) + i d^{-1} V d_i (\Gamma^P \Gamma^P) + i(\Gamma^P \Gamma^P) d_i V d^{-1} \\
&\quad - d^{-1} V d_i V d^{-1} - 4i d^{-1} V d_i L - 4i L d_i V d^{-1} - i d^{-1} V d_i (GG) - i(GG) d_i V d^{-1}.
\end{aligned} \tag{6.38}$$

Then if, according to the intrinsic PT algorithm, we discard from Eqs.(6.33) and (6.38) the terms proportional to the external inverse propagator, we find

$$\begin{aligned}\Pi'_{\alpha\beta}{}^{\text{IP}(2)}(q) &= -i\mathbb{I}_{A_\alpha A_\rho}^{(1)}(q)V_\beta^{\text{P}(1)\rho}(q), \\ S'_{\alpha\beta}{}^{\text{IP}(2)}(q) &= -q^2 I_2 P_{\alpha\beta}(q) + i\mathbb{I}_{A_\alpha A_\rho}^{(1)}(q)V_\beta^{\text{P}(1)\rho}(q),\end{aligned}\tag{6.39}$$

so that adding by parts the equations above we obtain

$$R_{\alpha\beta}{}^{\text{IP}(2)}(q) = -q^2 I_2 P_{\alpha\beta}(q).\tag{6.40}$$

Thus, finally, the quantity $-\Pi_{\alpha\beta}{}^{\text{IP}(2)}(q) + R_{\alpha\beta}{}^{\text{IP}(2)}(q)$ will provide precisely the expressions appearing in the two-loop version of the relevant BQI, *i.e.*, Eq.(5.11); or, equivalently, Eq.(6.20) is proved. Notice that if instead of resorting to the BQI one were to attempt a direct comparison of the answer to the two-loop BFM gluon self-energy, one would have to: *(i)* collect the pieces denoted by ellipses in Eq.(6.27); *(ii)* add them to the first and fourth term of Eq.(6.21); *(iii)* add the $R_{\alpha\beta}{}^{\text{IP}(2)}(q)$ of Eq.(6.40)– at that point we have the PT result of Eq.(6.19). *(vi)* To compare the answer to that of the BFM we need to algebraically manipulate the result; most notably one must recover the very characteristic ghost structure emerging in the BFM framework, and in particular the appearance of four-particle ghost-vertices. This straightforward but laborious procedure of algebraically recovering from the PT answer all the individual Feynman diagrams appearing in the BFM has been followed in the original two-loop presentation [23, 24], in the context of the S -matrix PT.

VII. CONCLUSIONS

In this paper we have formulated for the first time the PT not in terms of the elementary WI satisfied by the bare, tree-level vertices of the theory, but instead in terms of the STI satisfied by the higher order (one-loop and higher) vertices. In particular, the STI satisfied by the one-loop three-gluon vertex allows one to take a first step towards a non-diagrammatic implementation of the PT algorithm: instead of manipulating *individual* Feynman diagrams, entire sets of such diagrams are treated at once. In particular, the pieces that are reassigned from the vertices to the self-energies (or vice-versa) can be collectively identified with the ghost Green's functions appearing in the STI; these ghost Green's functions determine the deviation of the STI from the naive, tree-level WI. In order to avoid possible confusions we

emphasize that the STI are employed for the subset of diagrams nested inside the higher order loops, in the conventional formulation; however, the final one- and two-loop effective PT Green's functions obtained through this procedure do not satisfy STIs but instead the characteristic naive, QED-like WIs known from the earlier literature on the subject [1, 2].

For comparing the PT results to those of the BFM, we have employed a set of identities relating the conventional Green's functions to the corresponding ones in the BFM; the two sets are related by means of auxiliary Green's functions built from background sources and anti-fields, which are characteristic of the BV formalism we have employed for arriving at them. It turns out that these auxiliary Green's functions are connected to the ghost Green's functions appearing in the STI by Eq.(3.23). It is interesting that even though they originate from entirely different formalisms, the two sets of unphysical Green's functions are related by such simple expressions. Quite remarkably, the PT exposes these underlying relations, which appear to be encoded, in a non-manifest and very intricate way, into physical observables, such as S -matrix elements.

It is worth reviewing briefly some of the main physical application of the PT in the context of QCD. The unambiguous construction [47, 48, 49] of the universal (process-independent), gauge-fixing-parameter-independent, scale- and scheme-invariant effective charge is of significant interest [1, 2, 3, 50]. This PT construction allows for the explicit identification of the conformally-(in)variant subsets of QCD graphs [51, 52, 53]. This is of relevance in the field of renormalon calculus, where one studies the onset of non-perturbative effects from the behaviour near the QCD mass-scale of appropriately selected infinite sub-sets of the perturbative series [54].

The systematic study of the interface between perturbative and non-perturbative QCD is a long-standing problem. It has been advocated that the non-perturbative QCD effects can be reliably captured at an inclusive level by means of an infrared finite quantity, which would constitute the extension of the perturbative QCD running coupling to low energy scales [55]. Early results [1] based on the study of gauge-invariant Schwinger-Dyson equations involving this quantity suggest that such a description can in fact be derived from first principles. According to this analysis, the self-interaction of gluons give rise to a dynamical gluon mass, while preserving at the same time the local gauge symmetry of the theory. The presence of the gluon mass saturates the running of the QCD coupling; so, instead of increasing indefinitely in the infrared as perturbation theory predicts, it “freezes” at a finite value

[1, 2, 3]; for an interesting discussion on the phenomenological implications of the various “freezing” models and mechanisms available in the literature, see [56].

Finally, as has been pointed out by Brodsky in a series of recent papers [57, 58, 59], the PT effective charge can serve as the natural scheme for defining the coupling in the proposed “event amplitude generators” based on the the light-cone formulation of QCD.

It is interesting to extend the analysis presented here for the case of QCD to the more involved context of theories with spontaneous symmetry breaking, in general, and the Electroweak Sector of the Standard Model in particular. A detailed analysis [60] reveals that the BV formalism is particularly suited for accomplishing the two-loop generalization of the PT in the Electroweak Sector, a task which, due to the proliferation of Feynman diagrams and the non-transversality of the gauge boson self-energies, has been pending.

We believe that the methodology and the formal connections established in this paper set up the stage for the formulation of the PT to all orders in perturbation theory [26]. It remains to be seen whether the PT will transcend its humble diagrammatic origins and acquire the stature of a well-defined formal tool.

Acknowledgments

D.B. acknowledges useful correspondence with G. Barnich and T. Hurth. J.P. thanks P.A. Grassi for various valuable discussions and communications. The work of D.B. is supported by the Ministerio de Ciencia y Tecnología, Spain, under Grant BFM2001-0262, and the research of J.P. is supported by CICYT, Spain, under Grant AEN-99/0692.

-
- [1] J. M. Cornwall, Phys. Rev. **D26**, 1453 (1982).
 - [2] J. M. Cornwall and J. Papavassiliou, Phys. Rev. **D40**, 3474 (1989).
 - [3] J. Papavassiliou, Phys. Rev. **D41**, 3179 (1990).
 - [4] A. A. Slavnov, Theor. Math. Phys. **10**, 99 (1972).
 - [5] J. C. Taylor, Nucl. Phys. **B33**, 436 (1971).
 - [6] J. Papavassiliou and A. Pilaftsis, Phys. Rev. Lett. **75**, 3060 (1995), arXiv:hep-ph/9506417.
 - [7] J. Papavassiliou and A. Pilaftsis, Phys. Rev. **D53**, 2128 (1996), arXiv:hep-ph/9507246.
 - [8] B. S. Dewitt, Phys. Rev. **162**, 1195 (1967).

- [9] J. Honerkamp, Nucl. Phys. **B48**, 269 (1972).
- [10] R. E. Kallosh, Nucl. Phys. **B78**, 293 (1974).
- [11] H. Kluberg-Stern and J. B. Zuber, Phys. Rev. **D12**, 482 (1975).
- [12] I. Y. Arefeva, L. D. Faddeev, and A. A. Slavnov, Theor. Math. Phys. **21**, 1165 (1975).
- [13] G. 't Hooft, in **Karpacz 1975, Proceedings, Acta Universitatis Wratislaviensis* (Wroclaw, 1976), vol. 1, No. 368, pp. 354–369.
- [14] L. F. Abbott, Nucl. Phys. **B185**, 189 (1981).
- [15] S. Weinberg, Phys. Lett. **B91**, 51 (1980).
- [16] G. M. Shore, Ann. Phys. **137**, 262 (1981).
- [17] L. F. Abbott, M. T. Grisaru, and R. K. Schaefer, Nucl. Phys. **B229**, 372 (1983).
- [18] C. F. Hart, Phys. Rev. **D28**, 1993 (1983).
- [19] S. Weinberg, *The Quantum Theory of Fields*, vol. II (Cambridge University Press, New York, 1996).
- [20] A. Denner, G. Weiglein, and S. Dittmaier, Phys. Lett. **B333**, 420 (1994), arXiv:hep-ph/9406204.
- [21] S. Hashimoto, J. Kodaira, Y. Yasui, and K. Sasaki, Phys. Rev. **D50**, 7066 (1994), arXiv:hep-ph/9406271.
- [22] A. Pilaftsis, Nucl. Phys. **B487**, 467 (1997), arXiv:hep-ph/9607451.
- [23] J. Papavassiliou, Phys. Rev. Lett. **84**, 2782 (2000), arXiv:hep-ph/9912336.
- [24] J. Papavassiliou, Phys. Rev. **D62**, 045006 (2000), arXiv:hep-ph/9912338.
- [25] J. S. Ball and T.-W. Chiu, Phys. Rev. **D22**, 2550 (1980).
- [26] D. Binosi and J. Papavassiliou, in preparation.
- [27] C. Becchi, A. Rouet, and R. Stora, Commun. Math. Phys. **42**, 127 (1975).
- [28] C. Becchi, A. Rouet, and R. Stora, Annals Phys. **98**, 287 (1976).
- [29] I. V. Tyutin (1975), Lebedev Institute preprint 75-39.
- [30] P. Pascual and R. Tarrach, *QCD: Renormalization for the Practitioner* (Springer and Verlag, Heydelberg, 1984).
- [31] I. A. Batalin and G. A. Vilkovisky, Phys. Rev. **D28**, 2567 (1983).
- [32] I. A. Batalin and G. A. Vilkovisky, Phys. Lett. **B69**, 309 (1977).
- [33] P. Gambino and P. A. Grassi, Phys. Rev. **D62**, 076002 (2000), arXiv:hep-ph/9907254.
- [34] P. A. Grassi, T. Hurth, and M. Steinhauser, Nucl. Phys. **B610**, 215 (2001), arXiv:hep-

- ph/0102005.
- [35] G. Barnich, F. Brandt, and M. Henneaux, Phys. Rept. **338**, 439 (2000), arXiv:hep-th/0002245.
 - [36] G. Barnich and P. A. Grassi, Phys. Rev. **D62**, 105010 (2000), hep-th/0004138.
 - [37] P. A. Grassi, T. Hurth, and M. Steinhauser, Annals Phys. **288**, 197 (2001), arXiv:hep-ph/9907426.
 - [38] We are grateful to P. A. Grassi for pointing this out and for kindly furnishing to us the details for their derivation.
 - [39] D. Binosi and J. Papavassiliou, Phys. Rev. **D65**, 085003 (2002), hep-ph/0110238.
 - [40] Y. L. Dokshitzer, D. Diakonov, and S. I. Troian, Phys. Rept. **58**, 269 (1980).
 - [41] A. Andrasi and J. C. Taylor, Nucl. Phys. **B192**, 283 (1981).
 - [42] D. M. Capper and G. Leibbrandt, Phys. Rev. **D25**, 1002 (1982).
 - [43] G. 't Hooft, Nucl. Phys. **B33**, 173 (1971).
 - [44] J. M. Cornwall and G. Tiktopoulos, Phys. Rev. **D15**, 2937 (1977).
 - [45] N. J. Watson, Phys. Lett. **B349**, 155 (1995), arXiv:hep-ph/9412319.
 - [46] N. J. Watson, Nucl. Phys. **B552**, 461 (1999), arXiv:hep-ph/9812202.
 - [47] G. Grunberg, Phys. Rev. **D40**, 680 (1989).
 - [48] G. Grunberg, Phys. Rev. **D46**, 2228 (1992).
 - [49] R. Haussling, E. Kraus, and K. Sibold, Nucl. Phys. **B539**, 691 (1999), arXiv:hep-th/9807088.
 - [50] N. J. Watson, Nucl. Phys. **B494**, 388 (1997), arXiv:hep-ph/9606381.
 - [51] S. J. Brodsky, E. Gardi, G. Grunberg, and J. Rathsmann, Phys. Rev. **D63**, 094017 (2001), arXiv:hep-ph/0002065.
 - [52] J. Rathsmann (2001), arXiv:hep-ph/0101248.
 - [53] S. J. Brodsky, G. P. Lepage, and P. B. Mackenzie, Phys. Rev. **D28**, 228 (1983).
 - [54] S. Peris and E. de Rafael, Nucl. Phys. **B500**, 325 (1997), arXiv:hep-ph/9701418.
 - [55] Y. L. Dokshitzer, G. Marchesini, and B. R. Webber, Nucl. Phys. **B469**, 93 (1996), arXiv:hep-ph/9512336.
 - [56] A. C. Aguilar, A. Mihara, and A. A. Natale, Phys. Rev. **D65**, 054011 (2002), arXiv:hep-ph/0109223.
 - [57] S. J. Brodsky (2001), arXiv:hep-ph/0111127.
 - [58] S. J. Brodsky, Acta Phys. Polon. **B32**, 4013 (2001), arXiv:hep-ph/0111340.
 - [59] S. J. Brodsky (2001), arXiv:hep-th/0111241.

[60] D. Binosi and J. Papavassiliou (2002), hep-ph/0204308.